# Chapter 2
# Prebreakdown Air Ionization in the Atmosphere

**N.V. Ardelyan, Vladimir L. Bychkov, I.V. Kochetov, and K.V. Kosmachevskii**

**Abstract** This chapter is devoted to the analysis of electron-ionization and -elimination processes at early stages of electric-discharge development in air at altitudes of mainly 0–90 km. In this chapter, ionization processes in an external electric field, as well as background ionization by fast particles and electron attachment and detachment with participation of atomic and molecular oxygen, are considered. Temperature and concentration dependences of rate constants are described. Analysis of ionization models allowing simplified approaches to detailed computation models is undertaken. It is shown that the electric breakdown process in air, under the influence of an external electric field, comprises several stages that are different with respect to different altitudes over the Earth. Numerical modeling on the basis of a detailed plasma chemical model, taking into account the heating of gas by the discharge, has shown that the relaxation processes leading to gas

N.V. Ardelyan • K.V. Kosmachevskii
Computational Mathematics and Cybernetics Department,
M.V. Lomonosov Moscow State University, Moscow, Russia
e-mail: ardel@cs.msu.su; kosma@cs.msu.su

V.L. Bychkov (✉)
Department of Physical, M.V. Lomonosov Moscow State University, Moscow, Russia

Plasma – Chemistry Laboratory, FSUE "Moscow Radiotechnical Institute of RAS", Moscow, Russia
e-mail: bychvl@gmail.com

I.V. Kochetov
State Research Center of Russian Federation, Troitsk Institute for Innovation and Fusion Research, Moscow, Russia

V. Bychkov et al. (eds.), *The Atmosphere and Ionosphere: Elementary Processes, Monitoring, and Ball Lightning*, Physics of Earth and Space Environments,
DOI 10.1007/978-3-319-05239-7_2, 

heating also lead to the appearance of a nonlinear stage of electric breakdown. The considered phenomena can be convenient in the consideration of a high-altitude origination of natural discharges in fields of thunderstorm clouds.

**Keywords** Ionization • Attachment • Detachment • Breakdown • Gas discharge • Elementary processes • Models of the ionization • Chemical kinetics model • Atmosphere • Mesosphere

## 2.1 Introduction

Practical problems of electric-discharge devices applied in air at different altitudes requires knowledge of ionization thresholds because ionization is a source of charged particles in plasma and thus determines the efficiency of the applied devices (Raizer 1991; Aleksandrov et al. 2008). Therefore, the solution to ionization-threshold determination in electric-discharge devices at a given altitude actually comes connected to a set of applications and stimulates investigations devoted to these questions.

From data available in the literature, it is known that the development of discharge in air has been well described with respect to processes of origination and elimination of electrons in direct ionization, attachment, detachment, and other processes (Akishev et al. 1994). Determination of effective ionization thresholds requires the rate constants of corresponding processes to be determined with sufficiently high accuracy in the vicinity of the ionization threshold. This condition requires clarification (on the basis of experimental measurements or calculations on the basis of solution of the Boltzmann equation to determine an Electron-Distribution Function over Energies (EDFE), and the subsequent integration of electron-molecule process cross sections with EDFE) the rate- constant values of the basic processes.

Nevertheless, there exist many questions about the initial stage of ionization in air under real conditions. According to the work of (Aleksandrov et al. 2011), which was devoted to the research of ionization processes in the troposphere at altitudes of 4–12 km, it was shown that the measured breakdown of air electric field strength is approximately $\leq$3 V/cm, which is considerably lower than the breakdown of electric field strength near the surface of the Earth. In the work of (Bychkov et al. 2004), which discusses questions of ionization in the longitudinal discharge in a stream of air, there are breakdown fields considerably smaller than those near the Earth. Research results of ionization processes at higher altitudes where ionization processes can take place, leading to electric discharge phenomena, such as sprites, jets, *etc*. (Khodataev 2013; Raizer et al. 1998) are of great interest.

The purpose of this chapter is the consideration of a prebreakdown stage of discharge development in air; determination of the dependence of ionization in

air on a value of the reduced electric field ($E/N$ where $E$ is the electric field strength, and $N$ is the concentration of neutral particles of the gas); and determination of ionization threshold in dry air at different altitudes above the Earth. Values of the $E/N$ parameter will be compared with those that are typical for glow discharges.

A brief section of this review is devoted to questions about the determination of electron-molecule rate constants on the basis of the Boltzmann equation solution. Modeling was performed for conditions close to those of the experiment.

Rate constants of ion-molecular processes, *i.e.*, processes with the participation of electronically excited molecules and chemical reactions, as a rule are determined from experimental works and theoretical data. Many works on the determination of these rate constants have been published; many tables and reviews are devoted to these processes. However, regarding the concrete conditions of modeling, it is not always possible to locate all of the required information, and it becomes necessary to use poorly proven interpolation and extrapolation. Gathering data on energy values (formation enthalpy) passing into gas or reaction products is extremely difficult from an unambiguous point of view under the nonequilibrium conditions of discharges. Often a check of those or other assumptions underlying the consecutive analysis, or a performance of complex model calculations, reveals difficulties of interpretation; in this case, simple models of a considered situation are helpful. Therefore, a separate section of this review is devoted to the analysis of such models. In this review, concrete examples of consecutive computations of gas-discharge plasma in dry air at different altitudes are presented.

## 2.2 Determination of Rate Constants on the Basis of Solution of the Boltzmann Equation

### *2.2.1 Equation for Electron-Distribution Function Over Energies*

To model the physical phenomena taking place in gas-discharge systems of different types, it is necessary to determine an electron-distribution function over energies (EFDE). EFDE in the electric field in a gas is described by the kinetic Bolzman equation (Shkarovsky et al. 1966). It has been postulated that EFDE expands into a series of spherical harmonics (Legendre polynomial). This consideration is usually limited by the two first terms of the expansion (the "two-term approximation"). The Boltzmann equation for the spherically symmetric part of EFDE $f(u)$ in the two-term approximation of one-component

gas for a constant in a time- and uniform-space electrical field has the following form (Raizer 1991):

$$\begin{aligned}
&\sqrt{\frac{m}{2e}}u^{\frac{1}{2}}f(u)\frac{\mathrm{d}n_e}{\mathrm{d}t}+\frac{1}{3}\left(\frac{E}{N}\right)^2\frac{d}{\mathrm{d}u}\left(\frac{u}{Q_m(u)}\frac{\mathrm{d}f(u)}{\mathrm{d}u}\right)\\
&\quad+\frac{2m}{M}\frac{d}{\mathrm{d}u}\left(u^2Q_m(u)\left(f(u)+\frac{kT}{e}\frac{\mathrm{d}f(u)}{\mathrm{d}u}\right)\right)+B\frac{d}{\mathrm{d}u}\left(u\sigma_R(u)\left(f(u)+\frac{kT}{e}\frac{\mathrm{d}f(u)}{\mathrm{d}u}\right)\right)\\
&\quad+\sum_{i=1}^{n}y_{1i}(u+u_i)f\left(u+u_i\right)Q_i\left(u+u_i\right)-uf\left(u\right)\sum_{i=1}^{n}y_{1i}Q_i\left(u\right)\\
&\quad+\sum_{i=1}^{n}y_{2i}(u-u_i)f\left(u-u_i\right)Q_{-i}\left(u-u_i\right)-uf\left(u\right)\sum_{i=1}^{n}y_{2i}Q_{-i}\left(u\right)\\
&\quad+(u+u_i)f\left(u+u_i\right)Q_{\mathrm{ion}}\left(u+u_i\right)-uf\left(u\right)Q_{\mathrm{ion}}\left(u\right)+\sqrt{\frac{m}{2e}}\delta\left(u\right)K_i-uf\left(u\right)Q_{\mathrm{att}}\left(u\right)=0,
\end{aligned}\tag{2.1}$$

where $E$ is the electric field strength; $N$ is the total density of neutral particles; $m$ and $M$-masses of the electron and a particle colliding with it, respectively, $u$ is electron energy; $Q_m(u)$ is the cross section of an electron's interaction with a particle; $T$ is the translational temperature of the gas; $B$ is a rotation constant; $\sigma_R(u)$ is the effective cross section of rotation-level excitation; $y_{1i}$ and $y_{2i}$ are relative concentrations of the initial and final state in $i$-th inelastic process; $u_i$ is the threshold of $i$-th inelastic process; $Q_i(u)$ and $Q_{-i}(u)$ are cross sections of excitation and de-excitation in $i$-th process; $K_i$ is a constant of ionization, is calculated using EFDE; and $\delta(u)$ is a delta function. This equation is easily generalized in the case of a mixture of several gases.

The first term in the equation describes the influence of the origination and elimination of electrons; the second term describes the energy gain of electrons in the electric field; and the third and the fourth terms represent losses of electrons energy at elastic collisions and excitation of rotational levels, respectively. The fifth and sixth terms are responsible for inelastic collisions of electrons with particles, and the seventh and eighth terms are responsible for super-elastic collisions of electrons with excited particles (second-order collisions). The ninth, tenth, and eleventh terms consider the process of ionization of a particle assuming that the second electron is born with zero energy. The 12th term considers the process of dissociative attachment of an electron to a particle. A similar term, "ion recombination," arises in the case of the dissociative electron.

From (2.1), one can see that EFDE is defined by a value of the reduced electric field $E/N$. For this value, a unit of measure called a "Townsend" (1 Td = 10 − 17 V cm$^2$) is usually used. A cross section of the de-excitation and excitation processes is connected by a principle of detailed balance as follows:

$$Q_{-i}(u) = \frac{g_{-i}}{g_i}\frac{u+u_i}{u}Q_i(u+u_i), \tag{2.2}$$

where $g_i$ and $g_{-i}$ are statistical weights of the corresponding states.

The excitation of rotation levels of molecules $N_2$ and $O_2$ is considered in the diffusion approximation. For nitrogen molecules, the effective cross section of rotation-level excitation is calculated by the following formula (Kochetov et al. 1979; Dyatko et al. 1992):

$$\sigma_R(u) = 6\sigma_{02}(u) + 20\sigma_{04}(u), \tag{2.3}$$

where $\sigma_{02}(u)$ and $\sigma_{04}(u)$ are cross sections of two- and four-quantum excitation of the rotation state from the state with the rotation quantum number $J = 0$.

For oxygen molecules, the effective cross section of rotation-level excitation is calculated by the following formula (Islamov et al. 1977):

$$\sigma_R(u) = 10\sigma_{13}(u) + 12\sigma_{15}(u), \tag{2.4}$$

where $\sigma_{13}(u)$ and $\sigma_{15}(u)$ are cross sections of two- and four-quantum excitation of the rotation state from the state with the rotation quantum number $J = 1$.

The normalizing condition used for EFDE is as follows:

$$\int_0^\infty \sqrt{u} f(u)\mathrm{d}u = 1. \tag{2.5}$$

A rate constant of excitation in the $i$-th process is calculated by the following formula:

$$K_i = \sqrt{\frac{2e}{m}}\int_0^\infty uQ_i(u)f(u)\mathrm{d}u. \tag{2.6}$$

The electron-drift velocity is calculated as follows:

$$V_d = -\sqrt{\frac{2e}{m}}\frac{1}{3}\frac{E}{N}\int_0^\infty \frac{u}{Q_m(u)}\frac{\mathrm{d}f(u)}{\mathrm{d}u}\mathrm{d}u. \tag{2.7}$$

The electron "temperature" is calculated by the following formula:

$$T_e = \frac{2}{3}\int_0^\infty u^{\frac{3}{2}} f(u)\mathrm{d}u \tag{2.8}$$

The coefficient of the transversal diffusion is calculated as follows:

$$D_T = \sqrt{\frac{2e}{m}}\frac{1}{3}\frac{1}{N}\int_0^\infty \frac{uf(u)}{Q_m(u)}\mathrm{d}u \tag{2.9}$$

The portion of the electron energy going to the $i$-th inelastic process is calculated by the following formula:

$$\eta_i = \frac{u_i K_i}{V_d E/N}. \tag{2.10}$$

The method of solving the Boltzmann equation for EDFE determination is represented in the work of (Dyatko et al. 1992). Differential equation (2.1) is replaced by a finite-difference scheme defined on a uniform mesh over the axis of energy. The system of the linear equations obtained was solved by the marching method with subsequent iterations over the right parts of the equations.

### 2.2.2 *Choice of Cross Sections*

The accuracy of rate-constant calculation of electronic processes is defined first of all by the correct choice of electron-scattering cross sections on all components of the plasma. The only reliable criterion of an estimation of the cross section's set of reliability is the agreement of the calculated kinetic coefficients, drift velocities, and coefficients of electron diffusion with data obtained at measurements in drift tubes (Huxley & Crompton 1974). This criterion is traditionally used for the correction of cross sections measured in beam experiments as proposed previously by Phelps (Frost and Phelps 1962). At determination of scattering cross sections by processing the experimental data in the drift tubes, special attention should be given to the accuracy of the numerical model used for the conditions of the experiment. In particular, one must take into account that the value of the same kinetic coefficients appears to be different for different formulations of the experiment. This effect becomes essential at (1) the motion of electrons in high electric fields or (2) the presence of strong electron attachment (Petrović et al. 2009). The set of the cross sections satisfying this procedure is called the "self-consistent" set. Such self-consistent sets of cross sections are known to have many atoms and molecules (see, for example, http://www.lxcat.laplace.univ.tlse.fr/; Napartovich and Kochetov 2011).

Cross sections of electron interaction with unexcited molecules of $N_2$, $O_2$, and $H_2O$ have been taken from the works of (Phelps and Pitchford 1985; Ionin et al. 2007; Yousfi et al. 1987), respectively. Cross sections of the rotation-level excitation of nitrogen, $\sigma_{02}(u)$ and $\sigma_{04}(u)$, used in formula (2.3) were taken from Itikawa and Mason (2005), and cross sections of the rotation-level excitation of the oxygen molecule, $\sigma_{13}(u)$, and $\sigma_{15}(u)$, used in formula (2.4) were taken from the work of (Oksyuk 1965).

Calculations of electron-drift velocity, the coefficient of their transversal diffusion, and the rate constants of ionization depending on the value of the reduced electric field $E/N$ in dry air (Alexandrov et al. 1981; Deminsky et al. 2013, are well elucidated using extensive experimental data on the measurement of these characteristics as represented in the reviews of (Dutton 1975; Gallagher et al. 1983). Note that for some inexplicable reason, the experimental data on measurements of electron-drift velocities in dry air (Nielsen and Bradbury 1937; Roznerski and Leja 1984), in the most important range of the reduced electric field $E/N$, *i.e.*, from 10 to $\leq$100 Td, have fallen out favor (Dutton 1975; Gallagher et al. 1983).

A portion of discharge power expended on the excitation of molecule rotation levels passes in the heat during several collisions. Therefore, the portion of power expended on elastic losses and excitation of rotation levels is called "direct" heating. Note that the set of cross sections for molecular nitrogen yields good agreement for the dependence of direct heating in pure nitrogen on the $E/N$ value and has been measured experimentally (Kochetov et al. 1979). The portion of direct heating in pure nitrogen becomes essential at $E/N < 10$ Td (Kochetov et al. 1979).

In the description of electron collision, electrons with vibrationally excited nitrogen molecules, transitions between various vibrational levels ($N_2(v=i) \leftrightarrow N_2(v'=j)$, $i=0,\ 1,\ldots,\ 8$, $j=i+1,\ \ldots,\ 8$), and elastic scattering of vibrationally excited molecules were considered. Values of the corresponding sections were selected according to (Aleksandrov et al. 1978). In the case of oxygen, the only transitions considered were $O_2(v=0) \leftrightarrow O_2(v'=j)$, $j=i+1,\ 2,\ 3$ because of the small values of vibrational cross sections such that those of backward processes were obtained from the principle of detailed balance.

### 2.2.3 Kinetic Coefficients for Hot, Dry, and Humid Air

Distributions of populations over vibrational levels of nitrogen and oxygen molecules were considered as Boltzmann distributions with given vibrational temperature $T_V$ equal to the translational temperature of the gas. Air was modeled by the mixture of $N_2$:$O_2 = 4$:1.

In Fig. 2.1, one can see a dependence of drift velocity and electron temperature on $E/N$ in dry air at different translational temperatures of gas equal to 300, 1,000 and 1,500 K. Regarding differences in electron-drift velocities, their temperatures start only at low values of the reduced electric field, *i.e.*, $E/N < 3$ Td.

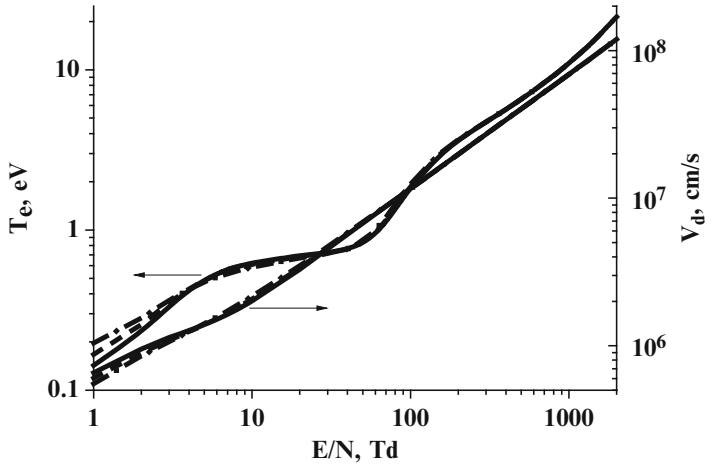


**Fig. 2.1** Dependence of electron-drift velocity and electron temperature on *E*/*N* in air for various gas temperatures. *Continuous line* 300 K, *dotted line* 1,000 K, *dash-dotted line* 1,500 K

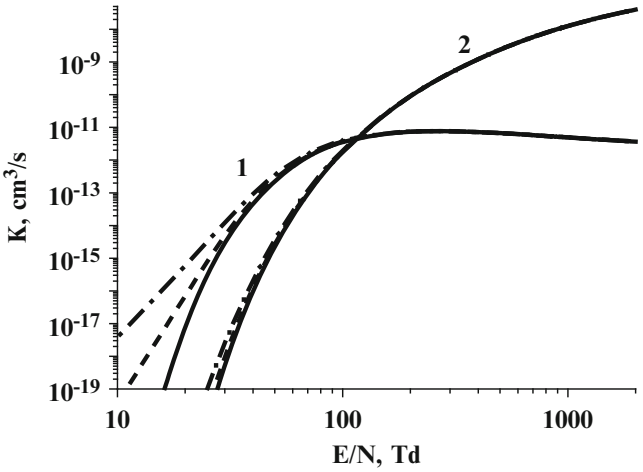


**Fig. 2.2** Dependence of dissociative recombination and ionization rate constants on *E*/*N* in air for various gas temperatures. *Continuous line* 300 K, *dotted line* 1,000 K, *dash-dotted line* 1,500 K

Figure 2.2 represents the dependence of total ionization on *E*/*N* in dry air at the same temperatures shown in Fig. 2.1. The rate constant of the dissociative attachment represented in Fig. 2.2 is multiplied by the relative concentration of $O_2$, and the total speed of ionization is calculated as the sum of ionization constants of separate components multiplied by the corresponding relative concentrations. Appreciable distinction from temperature begins at $E/N < 40$ Td.

Often seen as the term "breakdown field" (see discussion later in the text), this value is taken when the ionization frequency of molecules in the gas mixture

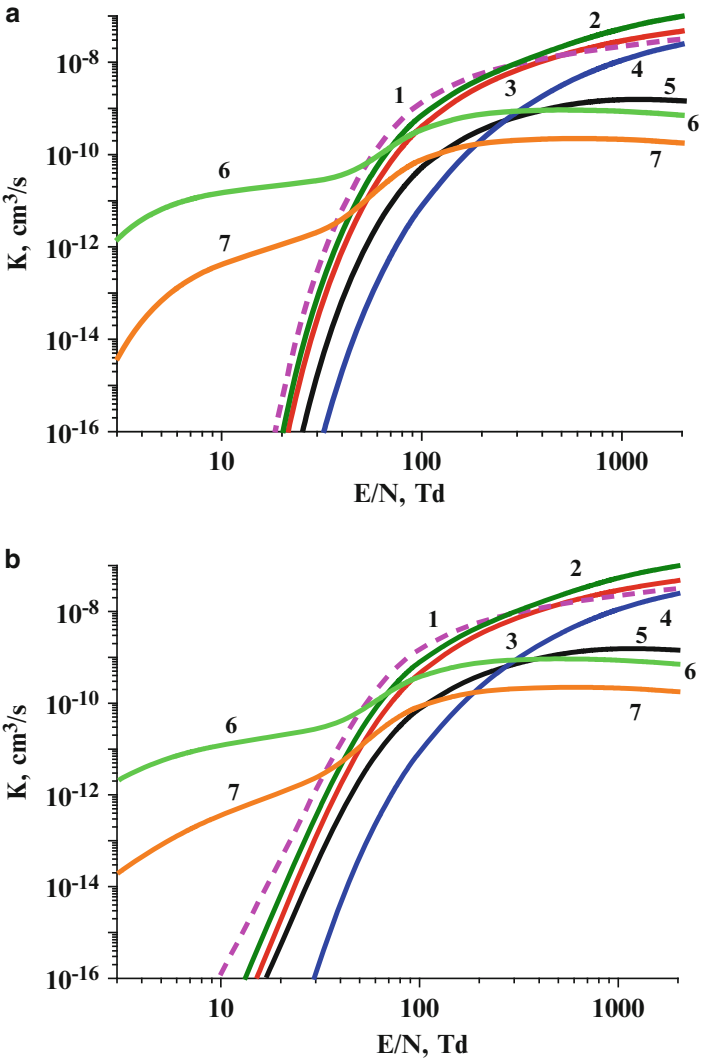


**Fig. 2.3** Dependence of dissociation and electronic-level excitation-rate constants on *E/N* in air for various gas temperatures. (**a**) 300 K. (**b**) 1,500 K. *1* dissociation of $O_2$, *2* dissociation of $H_2O$ molecules, *3* summed rate constant of excited-level nitrogen molecule above level $A^3\Sigma^+_u$, *4* dissociation of $N_2$, *5* excitation of level $A^3\Sigma^+_u$ of $N_2$, *6* and *7* excitation of levels $a^1\Delta_g$ and $b^1\Sigma_g^+$, respectively, of $O_2$.

becomes equal to that of the electron dissociative attachment to oxygen molecules; let us call it "conditional breakdown." At gas temperatures <1,500 K, the "breakdown" value of *E/N* does not vary and equals 115 Td.

To model plasma chemical processes, the dissociation of different components and the excitation of different long-lived electronic molecule levels are of particular interest. In Fig. 2.3, the dissociation rate constants of $N_2$, $O_2$, and $H_2O$ molecules

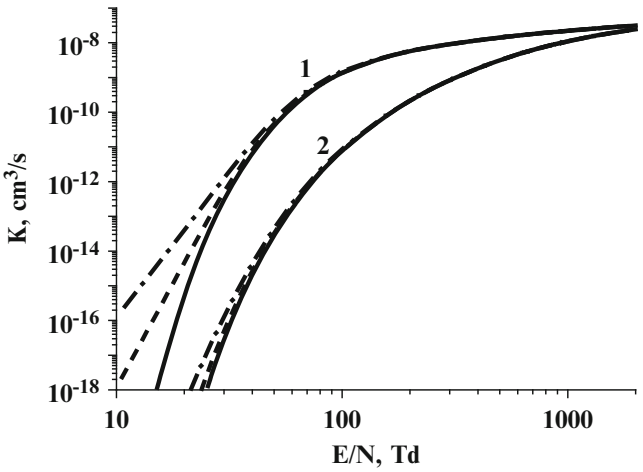


**Fig. 2.4** Dependence of dissociation rate constants of $O_2$ and $N_2$ molecules on *E/N* in air. *Continuous line* 300 K, *dotted line* 1,000 K, *dash-dotted line* 1,500 K

are presented. In such calculations, the concentration of water vapors chosen was small and did not influence EDFE. In the same figure, the excitation rate constant of an electronic state of nitrogen molecule $A^3\Sigma^+_u$, as well as the sum of excitation rate constants of other electronic levels of the nitrogen molecule, is represented. Here one can see the excitation rate constants of two lower electronic levels, $a^1\Delta_g$ and $b^1\Sigma_g{}^+$, of the oxygen molecule. Calculations are performed for two temperatures: 300 and 1,500 K.

Figure 2.4 shows the dependence of dissociation rate constants of oxygen and nitrogen molecules on *E/N* for temperatures 300, 1,000, and 1,500 K. An influence of gas temperature on the dissociation speed of $O_2$ molecules is noticeably stronger than that for nitrogen molecules, and this occurs at $E/N < 40$ Td. This is connected with the fact that such influence occurs due to the interaction of electrons with vibrationally excited nitrogen molecules.

Figure 2.5 shows the balance of energy of electrons in dry air. An appreciable change of electron energy balance at changes of gas temperature from 300 to 1,500 K takes place at $E/N < 30$ Td.

Figure 2.6 shows the dependence of electron-drift velocity and electron mean energy on electric field *E/N* in air with the addition of 0.5, 1, and 4 % water vapors. Distinctions among electron-drift velocities and their mean energy for different concentration of water arise only at fields <20 Td where an appreciable contribution to the electron energy balance begins to generate the excitation of vibrationally excited water molecules (see Fig. 2.7).

Figure 2.7 shows the portion of electron energy going to the excitation of vibrational levels, dissociation, dissociative attachment, and ionization of water molecules in air depending on a value of *E/N* at concentrations of water vapors of 0.5, 1, and 4 %. The maximal portion of electron energy going to the dissociation of water molecules is approximately 2.3 % at the reduced electric field of 270 Td at a water-molecule concentration of 4 %.

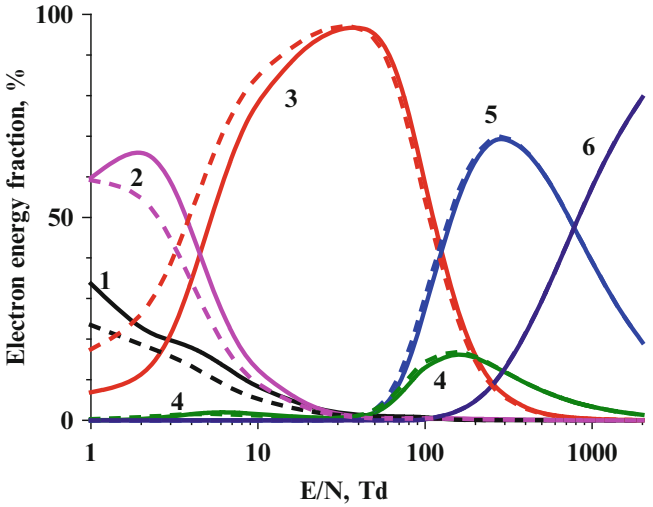


**Fig. 2.5** Balance of electron energy in air with respect to *E*/*N*. *1* elastic losses and excitation of rotational levels, *2* excitation of vibrations in $O_2$, *3* excitation of vibrations in $N_2$, *4* excitation of electronic levels in $O_2$, *5* excitation of electronic levels in $N_2$, *6* ionization. *Continuous line* gas temperature 300 K, *dotted line* 1,500 K

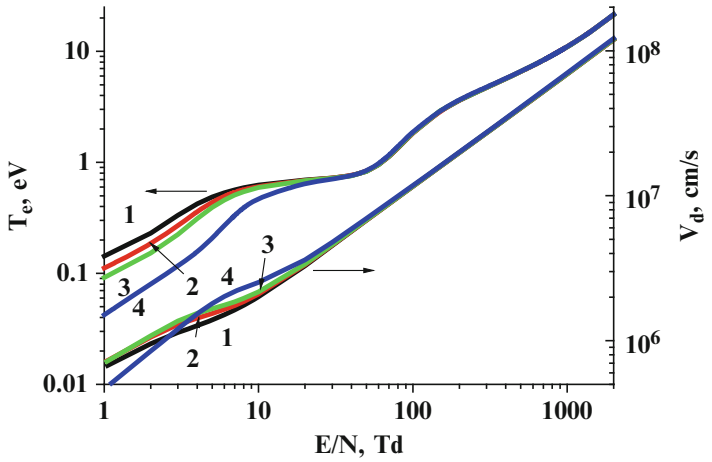


**Fig. 2.6** Dependence of electron-drift velocity and electron temperature on *E*/*N* in air at different concentrations of water molecules. *1* 0 %, *2* 0.5 %, *3* 1 %, *4* 4 % (various gas temperatures). $T = 300$ K

Dependence of the summed rate constants of dissociative attachment and ionization with respect to the reduced electric field *E*/*N* in dry air, as well as its mixture with approximately 4 % water vapors, is shown in Fig. 2.8. This figure presents the summed rate constants of dissociative attachment and the sum of rate

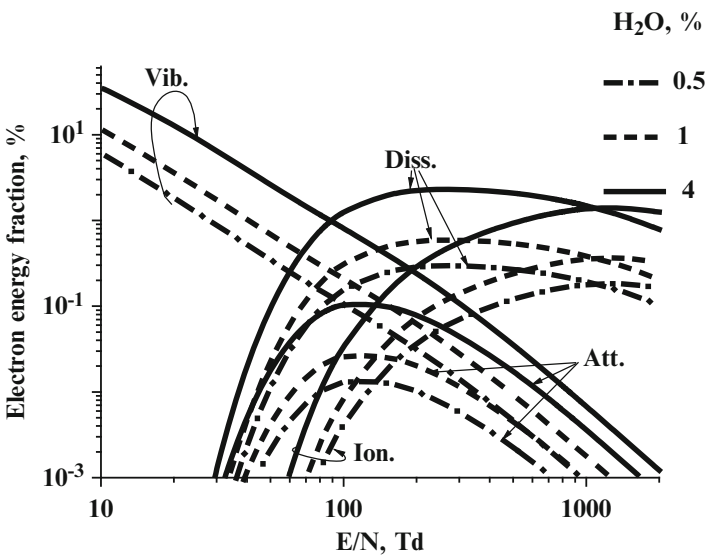


**Fig. 2.7** Portions of electron energy going to the excitation of different levels of freedom of water vapors with respect to *E/N* of different mixtures of water vapor and air. $T = 300$ K

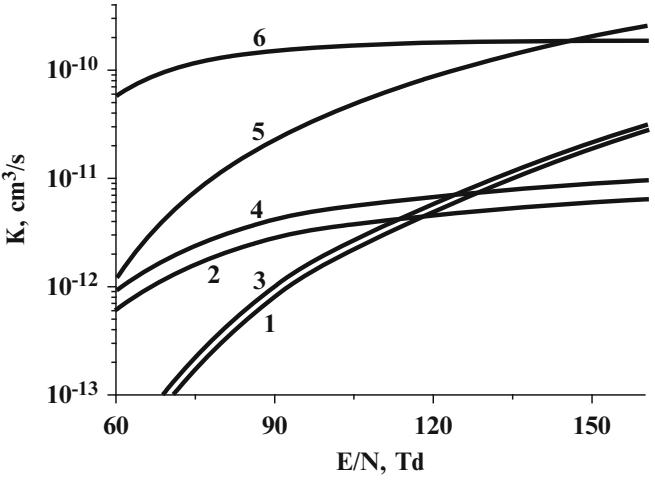


**Fig. 2.8** Rate constants of ionization (*1*, *3*, and *5*) and dissociative attachment (*2*, *4*, and *6*) with respect to *E/N* for different concentrations of water vapors. *1* and *2* dry air, *3* and *4* air with 4 % water vapors, *6* pure water vapors. $T = 300$ K

constants of dissociative attachment to oxygen and water molecules with weights corresponding to their relative concentrations. Similar summation over all components of the gas mixture is performed for the total rate constant of ionization represented in Fig. 2.8. Also shown are the rate constant of dissociative attachment

and ionization depending on $E/N$ in "pure" water vapors. With addition of 4 % water vapors to dry air, the value of the conditional breakdown $E/N$ increases from 115 to 124 Td. Note that the conditional breakdown $E/N$ value is 146 Td in pure water vapors. In calculations of the dissociative attachment of electrons to water molecules, the formation of negative ions $H^-$ and $O^-$ (Yousfi et al. 1987) is described. The channel of dissociative attachment with formation of negative ion $OH^-$ is neglected. Such an approach is justified because the value of the cross section of the electron dissociative attachment with formation of $OH^-$ is approximately 1.5 orders of magnitude smaller than attachment with the formation of $H^-$ (Itikawa and Mason 2005).

## 2.3 Ionization of Dry Air: Qualitative Analysis

At the beginning of the analysis, we will consider simple models of ionization allowing us to qualitatively analyze typical ionization-processes development at electric discharge in air and to show a transition to breakdown, *i.e.*, the ionization avalanche. One should consider this phenomenon together with background ionization and a number of electron-elimination and ion charge-exchange processes.

We analyze models described by systems of linear ordinary differential equations, the solution of which easily yields qualitative analytical results. Therefore, we consider only plasma chemical reactions of separate plasma components with main molecules, $O_2$ and $N_2$, the concentration of which does not vary substantially in low ionized plasma; in an approximation of the constancy of concentrations, the models are linear. Namely, such reactions prevail at the initial stage of ionization processes because of the high concentration of air molecules compared with that of plasma components. Models of recombination processes are nonlinear because at least two plasma components participate in the corresponding reactions; therefore, these processes cannot be considered in the qualitative linear analysis. However, the recombination processes are insignificant at the initial stages of the ionization process due to prevailing reactions with air molecules, the concentrations of which are many orders of magnitude greater than those of plasma components participating in recombination. Because of this, the considered models are adequate at the initial stage of ionization when plasma is low ionized and nonlinear recombination processes are insignificant.

Let us also specify that in the analysis of linear models of discharge ionization, we consider only key processes that as a rule prevail in the presence of substantial electric fields. A basic contribution to the formation of the background (not discharge) plasma can generate some other processes in small background electric fields and background ionization by fast particles. In small background electric fields, background ionization by fast particles forms a basic contribution to the formation of the background (not discharge) plasma, which can generate some other processes.

### 2.3.1 The Simplest Models

#### Direct Ionization and Dissociative Attachment

Usually the processes of ionization and attachment in air—*i.e.*, direct ionization of molecules by slow plasma electrons (originated in the discharge) and dissociative electron attachment to oxygen molecules—are considered together. The direct ionization of $O_2$ and $N_2$ molecules by slow electrons $e$ (Raizer 1991) takes place according to the following reaction formula:

$$e + O_2 \rightarrow O_2^+ + 2e, \quad e + N_2 \rightarrow {N_2}^+ + 2e, \tag{2.11}$$

with the creation of ${O_2}^+$ and ${N_2}^+$ ions and slow plasma electrons $e$.

Dissociative attachment of electrons to $O_2$ molecules with creation of negative ion $O^-$ and oxygen atoms takes place in correspondence with the following formula:

$$e + O_2 \rightarrow O^- + O. \tag{2.12}$$

At this stage of prebreakdown ionization, the influence of recombination processes is insignificant; therefore, one can disregarded them in models of prebreakdown ionization.

An ordinary differential equation describing a variation of the electron concentration in the course of processes (2.11) and (2.12) has the following form:

$$\frac{dN_e}{dt} = (\nu_i - \nu_a)N_e. \tag{2.13}$$

Here, $\nu_i = k_i(E/N) \cdot N$, $N = N_{N_2} + N_{O_2}$ is the total molecule concentration; $N_{N_2}$, $N_{O_2}$ are the concentrations of nitrogen and oxygen molecules, respectively; $k_i(E/N)$ is the rate constant of direct ionization process (2.11); and $\nu_a = k_a(E/N) \cdot N_{O_2}$, where $k_a(E/N)$ is the rate constant of dissociative attachment process (2.12).

A solution of (2.13) at the initial concentration of the electrons $N_{e0}$ is well known (Raizer 1991) as follows:

$$N_e = N_{e0}\exp((\nu_i - \nu_a)t). \tag{2.14}$$

One must determine the value of $N_{e0}$ from additional data. An obvious supposition that the condition $\nu_i \geq \nu_a$ yields a threshold value of the $E/N$ parameter at breakdown (referred to previously as "conditional breakdown") does not correspond with actual practice (Aleksandrov et al. 2008). Thus, the known breakdown value (in the sense of the appearance of an avalanche) of the electric field strength in air is equal to $E = 26$ kV/cm (Aleksandrov et al. 2008). However, the rate-constant data of ionization and dissociative recombination in air under normal conditions at application of the Boltzmann equation solution yield values of the conventional

breakdown of electric fields in the range of 29–32 kV/cm, and these values are different from the data of Raizer (1991). An account of other processes does not improve the situation because one must consider the initial concentration of all components participating in reactions. In addition, there exist questions about an opportunity of prebreakdown development of ionization when $\nu_i < v_a$ and other processes of electron appearance can take part.

Differential equations supplementing model (2.13) for the ion component of plasma look like this:

$$\frac{\mathrm{d}N_{M_2^+}}{\mathrm{d}t} = \nu_i N_e, \frac{\mathrm{d}N_{\mathrm{O}^-}}{\mathrm{d}t} = \nu_a N_e,$$

where $N_{M_2^+}$ is the concentration of positive ions of air molecules appearing in processes (2.11) of direct ionization, and $N_{\mathrm{O}^-}$ is the concentration of the ions $\mathrm{O}^-$ appearing in process (2.12) of dissociative attachment.

Taking into account the solution (2.14) the next formulas are obtained for ion concentrations valid at $\nu_i \neq v_a$ and at initial concentrations $N_{\mathrm{O}^-0}, N_{M_2^+0}$:

$$N_{\mathrm{O}^-} = \frac{\nu_a}{\nu_i - v_a} N_{e0}(\exp((\nu_i - v_a)t) - 1) + N_{\mathrm{O}^-0},$$
$$N_{M_2^+} = \frac{\nu_i}{\nu_i - v_a} N_{e0}(\exp((\nu_i - v_a)t) - 1) + N_{M_2^+0}.$$

It is evident here that at $\nu_i > v_a$ in the considered model, there is exponential growth of ions and electrons concentrations.

At $\nu_i < v_a$, electron concentrations, as defined by formula (2.14), tend to zero, but ion concentrations tend to constant values exceeding initial values as follows:

$$N_{\mathrm{O}^-} \underset{t\to\infty}{\to} \frac{\nu_a}{v_a - \nu_i} N_{e0} + N_{\mathrm{O}^-0}, \quad N_{M_2^+} \underset{t\to\infty}{\to} \frac{\nu_i}{v_a - \nu_i} N_{e0} + N_{M_2^+0}.$$

Such a behavior of ion concentration is one of the typical scripts in the case of a prevalence of electron-elimination processes over the processes of their origination. At any values of the initial data, plasma appears with a constant ion concentration.

### Background Ionization

It is well-known (Raizer 1991 Akishev et al. 1994; Sedunov 1991; Brasseur and Solomon 1984) that presence of charged particles in air under real conditions, in the absence of an electric field breakdown, is connected with background ionization by fast particles coming into the atmosphere from space and appearing in the atmosphere as a result of nuclear processes inside of the Earth. The atmospheric

background ionization by fast electrons $e'$ is described by the formula of reactions as follows:

$$e^{'} + O_2 \rightarrow O_2^{+} + e^{'} + e, \quad e^{'} + N_2 \rightarrow {N_2}^{+} + e^{'} + e, \tag{2.15}$$

and the differential equation describing a production of the slow electrons by the fast particles has the following form:

$$\frac{dN_e}{dt} = Q, \tag{2.16}$$

where $Q$ is a velocity of the process of the electron-ion pairs production depending on the velocity of initial particles and gas pressure (Raizer 1991; Sedunov 1991; Brasseur and Solomon 1984). This equation at the initial concentration of the electrons $N_{e0}$ has the following solution:

$$N_e = N_{e0} + Qt, \tag{2.17}$$

and at zero initial concentration determines electron production by the fast particles.

### Background Balance

In the absence of other sources of electrons in the atmosphere, the balance of charged particles—as defined by plasma chemical reactions describing the processes of ionization, recombination, attachment, detachment, and conversion, *etc*.—is established.

A simple evident model of such balance considers the processes (2.15) of ionization by fast particles, the process of three-body attachment of plasma electrons to molecules $O_2$ (Aleksandrov 1988)

$$e + O_2 + O_2 \rightarrow O_2^{-} + O_2 \tag{2.18}$$

with appearance of the negative ion ${O_2}^{-}$, and the process of ion–ion recombination (Smirnov 1974) as follows:

$$O_2^{-} + M_2^{+} \rightarrow O_2 + M_2, \tag{2.19}$$

where $M_2^{+}$ is a positive molecular ion.

The system of ordinary differential equations describing the change of a negatively charged plasma component in the course of processes (2.15), (2.18), and (2.19), looks like this:

$$\frac{dN_e}{dt} = Q - \nu_{tr} \cdot N_e, \tag{2.20}$$

$$\frac{dN_{o_2^-}}{dt} = \nu_{tr} \cdot N_e - \alpha \cdot N_{o_2^-} N_{M_2^+}, \tag{2.21}$$

where $\nu_{tr} = k_{tr} \cdot N_{O_2}^2$ is the frequency of process (2.18), $\alpha$ is a coefficient of ion–ion recombination, $N_{o_2^-}$ is the concentration of negative ion $O_2^-$, and $N_{M_2^+}$ is the concentration of ions $M_2^+$.

The establishment of balance corresponds to coming to a stationary state of the solution of the system (2.20), (2.21). Because the right-hand sides are close to zero $Q \approx \nu_{tr} N_e \approx \alpha N_{o_2^-} N_{M_2^+}$ and an accounting of plasma quasi-neutrality $N_{M_2^+} \approx N_{O_2^-} + N_e \approx N_{O_2^-} + Q/\nu_{tr}$ gives:

$$Q \approx \alpha \cdot N_{o_2^-} \left( N_{o_2^-} + Q/\nu_{tr} \right),$$

it follows that

$$N_{O_2^-} \approx \frac{1}{2\alpha} \left( -\frac{\alpha \cdot Q}{\nu_{tr}} + \sqrt{\left( \frac{\alpha \cdot Q}{\nu_{tr}} \right)^2 + 4\alpha \cdot Q} \right),$$

determines one of initial conditions variants for ionizing processes at the switching on of the electric field.

Under real conditions during a particular time period positive ions can change due to charge-exchange reactions, but the dependence for negative ions almost stays the same (see the calculations in section "Role of the background state" represented in Fig. 2.20 as curves for $N_e$, $N_{O_2^-}$, $N_{O_2^+}$ and $N_{NO^+}$).

### Background Ionization With Direct Ionization and Dissociative Attachment

Joint consideration of direct ionization processes by slow electrons (2.11), dissociative attachment (2.12), and background ionization (2.15) leads to the following differential equation for electron concentration:

$$\frac{dN_e}{dt} = Q + (\nu_i - \nu_a) N_e. \tag{2.22}$$

Equation (2.22) at initial electron concentration $N_{e0}$ and condition $\nu_i - \nu_a \neq 0$ have the following solution:

$$N_e = \frac{Q}{\nu_i - \nu_a} (\exp((\nu_i - \nu_a)t) - 1) + N_{e0} \exp((\nu_i - \nu_a)t). \tag{2.23}$$

In case of $\nu_i > v_a$ at large time values, the solution (2.23) yields the exponential growth of electron concentration (ionization avalanche) with velocity $\nu_i - v_a$. At zero initial concentration of electrons, the formation of plasma is conditioned by background ionization (2.13) and, in general, by both non-zero initial concentration and background ionization.

In case of $\nu_i < v_a$, different from model (2.13) of direct ionization and dissociative attachment, the electron concentration comes to the constant $Q/(v_a - \nu_i)$ with time conditioned by process (2.15) of background ionization by fast particles.

Equations describing the behavior of the ion concentration in (2.22) look like this:

$$\frac{\mathrm{d}N_{M_2^+}}{\mathrm{d}t} = Q + \nu_i N_e, \quad \frac{\mathrm{d}N_{\mathrm{O}^-}}{\mathrm{d}t} = \nu_a N_e,$$

At initial concentrations $N_{\mathrm{O}^-0}, N_{M_2^+0}$ under accounting of the solution (2.23), one obtains the following formulas for ion concentration $N_{\mathrm{O}^-}, N_{M_2^+}$:

$$N_{\mathrm{O}^-} = N_{\mathrm{O}^-0} + \frac{\nu_a}{(\nu_i - v_a)} \left[ \left( \frac{Q}{\nu_i - v_a} + N_{e0} \right) (\exp((\nu_i - v_a)t) - 1) - Qt \right],$$

$$N_{M_2^+} = N_{M_2^+0} + \frac{1}{(\nu_i - v_a)} \left[ \nu_i \left( \frac{Q}{\nu_i - v_a} + N_{e0} \right) (\exp((\nu_i - v_a)t) - 1) - \nu_a Qt \right].$$

It follows from these formulas that at $\nu_i > v_a$ the ions concentrations increase exponentially like to the electron concentration (2.13) decrease. In case of the attachment predominance ($\nu_i < v_a$) at long times the ion concentrations $N_{\mathrm{O}^-}, N_{M_2^+}$ increase linearly according to law $\dfrac{\nu_a Q}{v_a - \nu_i} t$, which is conditioned by background ionization (2.15).

### 2.3.2 Complication of the Model

Let us consider more complex model of prebreakdown ionization describing the secondary process of electrons appearance not reduced to one ordinary differential equation for electron concentration. For this purpose, alongside the processes of direct ionization (2.11), dissociative attachment (2.12), and background ionization (2.15), we consider the processes of electron detachment from negative ions $\mathrm{O}^-$ in air (Frost and Phelps 1962) as described by the formulas of reaction as follows:

$$\mathrm{O}^- + M \rightarrow e + \mathrm{O} + M, \tag{2.24}$$

$$\mathrm{O}^- + \mathrm{N}_2 \rightarrow e + \mathrm{N}_2\mathrm{O}. \tag{2.25}$$

Here, $M$ is a neutral particle in air, and $N_2$ and $N_2O$ are molecules participating in reactions.

In this case, the system of the chemical-kinetic equations for electrons and negative ions $O^-$ participating in direct and background ionization, becomes this:

$$\frac{dN_e}{dt} = Q + (\nu_i - v_a)N_e + \nu_{det}N_{O^-}, \tag{2.26}$$

$$\frac{dN_{O^-}}{dt} = v_a N_e - \nu_{det}N_{O^-}, \tag{2.27}$$

where $\nu_{det} = \nu_{det1} + \nu_{det2}$, $\nu_{det1} = k_{det1} \cdot N_M$, and $\nu_{det2} = k_{det2}N_{N_2}$ are frequencies of processes (2.24) and (2.25), and $N_M$ and $N_{N_2}$ are, respectively, concentrations of neutral components and nitrogen molecules.

The result of (2.26) and (2.27) is the second-order ordinary differential equation for electron concentration $N_e$:

$$\frac{d^2N_e}{dt^2} + (\nu_{det} - (\nu_i - \nu_a))\frac{dN_e}{dt} - \nu_{det}\nu_i N_e = \nu_{det}Q. \tag{2.28}$$

Roots of the characteristic equation for (2.28) are defined by the following formula:

$$\lambda_\pm = 0.5\left[((\nu_i - \nu_a) - \nu_{det}) \pm \sqrt{((\nu_i - \nu_a) - \nu_{det})^2 + 4\nu_{det}\nu_i}\right], \tag{2.29}$$

and partial solution $Y$ of inhomogeneous (2.28) is defined by the following formula:

$$Y = -Q/\nu_i. \tag{2.30}$$

Accounting for $\nu_i > 0, \nu_{det} > 0$ it follows from (2.29) that $\lambda_+ > 0, \lambda_- < 0$.

Because of (2.29) and (2.30), a general solution of differential equation (2.28) is given by this formula:

$$N_e = C_{e+}\exp(\lambda_+ t) + C_{e-}\exp(\lambda_- t) - Q/\nu_i. \tag{2.31}$$

At the given initial data $N_{e0}, N_{O^-0}$, constant $C_\pm$ can be determined from the system of the linear equations obtained at the account of the initial data and (2.26) at the initial moment of time as follows:

$$\begin{aligned} C_+ + C_- &= N_{e0} + Q/\nu_i, \\ C_+\lambda_+ + C_-\lambda_- &= Q + (\nu_i - \nu_a)N_{e0} + \nu_{det}N_{O^-}. \end{aligned} \tag{2.32}$$

From (2.32), it is obvious that constants $C_{\pm}$ depend on initial data, roots of the characteristic (2.29), and coefficients of the system of differential equations (2.26) and (2.27), *i.e.*, the rate constants of the considered processes.

Note that an analytic solution for ion $N_{O^-}$ concentration can be obtained from (2.26) with application of the solution for $N_e$. Let us also indicate that the concentration of ions satisfies the second-order ordinary differential equation (2.28) but does so with another right part as follows:

$$\frac{d^2N_{O^-}}{dt^2} + (\nu_{det} - (\nu_i - \nu_a))\frac{dN_{O^-}}{dt} - \nu_{det}\nu_i N_{O^-} = \nu_a Q, \tag{2.33}$$

the general solution of which is similar to (2.31):

$$N_{O^-} = C_{O^-+}\exp(\lambda_+ t) + C_{O^-_-}\exp(\lambda_- t) - \frac{\nu_a}{\nu_{det}\nu_i}Q, \tag{2.34}$$

where $C_{O^-\pm}$ are constants defined by initial data similar to (2.32).

From the point of view of qualitative analysis of analytical solution (2.31), it is interesting to note that solving system (2.32) it is easy to show that $C_{e+} > 0$. Expressing $C_{e-}$ through $C_{e+}$ from the first equation of system (2.32) and substituting the result into the second equation of (2.32), we obtain the following:

$$C_{e+}(\lambda_+ - \lambda_-) = Q\left(1 - \frac{\lambda_-}{\nu_i}\right) + [(\nu_i - \nu_a) - \lambda_-]N_{e0} + \nu_{det}N_{O^-0}.$$

From here, accounting for the negativity of $\lambda_-$, it follows that there is positivity of $C_{e+}$ at any non-negative initial data if $(\nu_i - \nu_a) - \lambda_- > 0$. The last inequality comes from the following transformations:

$$(\nu_i - \nu_a) - \lambda_- = 0.5\left[((\nu_i - \nu_a) + \nu_{det}) + \sqrt{((\nu_i - \nu_a) - \nu_{det})^2 + 4\nu_{det}\nu_i}\right]$$

$$= 0.5\left[((\nu_i - \nu_a) + \nu_{det}) + \sqrt{((\nu_i - \nu_a) + \nu_{det})^2 + 4\nu_{det}\nu_a}\right] > 0.$$

The positivity of $C_{e+}$ agrees with the physical sense because it ensures positivity of (2.31) at long times when the exponentially growing solution summand $C_{e+}\exp(\lambda_+ t)$ prevails, which in the physical sense indicates ionization avalanche.

More detailed analysis of the solution's positivity is beyond the framework of this chapter and is connected with a general theoretical question of the positivity of solutions to the Cauchy problem for systems of chemical kinetics equations, the final solution of which is currently unknown.

In concrete cases, without resorting to a detailed analysis of solutions like (2.31), it is possible to be convinced of the positivity of the solution graphically, having realized the analytical solution like (2.31) with the preliminarily found constant C

or solved numerically the Cauchy problem for the initial system of ordinary differential equations (2.26) and (2.27).

It is important to note that when considering a model, the consequence of the detachment processes present in (2.24) and (2.25) and the direct ionization in (2.11) ($\nu_{\text{det}}\nu_i > 0$) is the existence of the exponentially growing mode ($\lambda_+ > 0$) in the solution to (2.31), which is physically interpreted as the ionization avalanche as one can see from formula (2.29) in the roots of the characteristic equation. This fact does not depend on the ratio of direct ionization (2.11) and dissociative attachment (2.12) processes (a sign of $\nu_i - \nu_a$) unlike in the simpler models considered earlier. Phenomenologically, this fact can interpreted as absence of ionization threshold, which remains unproven by available experimental data. Therefore, consideration of a more complex models is expedient.

From (2.29), it also follows that increment $\lambda_+ > 0$ of the growing mode in the solution (2.31) at $\nu_i - \nu_a - \nu_{\text{det}} < 0$ can be so small that plasma concentration growth in the considered model will be insignificant in real physical time. Thereby, the value of $\lambda_+ > 0$ is also determinative from the point of view of identification of the ionization avalanche process.

### 2.3.3 *Model with Consideration of Electrons and Atomic and Molecular Oxygen Ions*

#### Formulation of the Model

Here we consider the model based on the system of reactions proposed in (Aleksandrov et al. 2011), which have been well recommended for the preliminary analysis of electic dicharge in cold and hot air. We consider that the concentration of electrons $N_e$ is defined by the following processes, which take place intensively in glow discharges at the ground level and in clouds: the direct ionization (2.11) of $O_2$ and $N_2$ molecules by slow electrons $e$; the atmospheric background ionization (2.15) by fast electrons $e'$; the dissociative attachment of electrons to molecules $O_2$ with creation of negative ion $O^-$ and atom O (2.12); the processes (2.20) and (2.21) of electron detachment from ions $O^-$; and the electron-detachment process from molecular ion $O_2^-$ at collisions with neutral molecules in air mixture as follows:

$$O_2^- + M \rightarrow e + O_2 + M \tag{2.35}$$

We also take into account that ions $O_2^-$ and $O_3^-$ appear when ion $O^-$ disappears in reactions as follows:

$$O^- + O_2 \rightarrow O_2^- + O, \tag{2.36}$$

$$O^- + O_2 + O_2 \rightarrow O_3^- + O_2. \tag{2.37}$$

In this model, unlike previously, we added process (2.35) of electron detachment from ion $O_2^-$ and processes (2.36) and (2.37) of ion $O^-$ elimination, which is the source of secondary electrons appearing in detachment processes (2.20) and (2.21).

The system of ordinary differential equations for electrons $N_e$ and negative ions $O^-$ and $O_2^-$ with concentrations $N_{O^-}$ and $N_{O_2^-}$ describing the indicated processes looks like this:

$$\frac{dN_e}{dt} = Q + (\nu_i - \nu_a)N_e + (\nu_{det1} + \nu_{det2})N_{O^-} + \nu_{det3}N_{O_2^-}, \tag{2.38}$$

$$\frac{dN_{O^-}}{dt} = \nu_a N_e - (\nu_{det1} + \nu_{det2} + \nu_{ch1} + \nu_{ch2})N_{O^-}, \tag{2.39}$$

$$\frac{dN_{O_2^-}}{dt} = \nu_{ch1}N_{O^-} - \nu_{det3}N_{O_2^-}. \tag{2.40}$$

Here $\nu_i = k_i N$, $N = N_{N_2} + N_{O_2}$ is the total concentration of molecules; $N_{N_2}$, $N_{O_2}$ are, respectively, concentrations of nitrogen and oxygen molecules; $k_i$ is the rate constant of direct ionization process (2.11); $Q$ is the rate constant of background ionization process (2.15); $\nu_a = k_a N_{O_2}$, $k_a$ is the rate constant of dissociative attachment process (2.12); $\nu_{det1} = k_{det1}N$, $k_{det1}$ is the rate constant of detachment process (2.20); $\nu_{det2} = k_{det2}N_{N_2}$, $k_{det2}$ is the rate constant of detachment process (2.21); $\nu_{det3} = k_{det3}N_{O_2}$, $k_{det3}$ is the rate constant of detachment process (2.35); $\nu_{ch1} = k_{ch1}N_{O_2}$, $k_{ch1}$ is the rate constant of charge-exchange process (2.36); and $\nu_{ch2} = k_{ch2}(N_{O_2})^2$, $k_{ch2}$ is the rate constant of conversion process (2.37).

In principle, coefficient $\nu_i - \nu_a$ can be both positive and negative; however from Fig. 2.9, it follows that this coefficient is always negative for air in the examined range of the $E/N$ parameter. This means that electric discharge in air (in frames of the considered model) occurs under conditions prevalent with the electron-elimination process (due to dissociative attachment (2.12)) over the process of their appearance (direct ionization (2.11)) when the elementary model (2.13) does not describe the breakdown and its initial stage, *i.e.*, ionization avalanche. In other words, this circumstance makes necessary the consideration of complicated models to explain the phenomenon of breakdown in air.

In the given model, as well as in the models examined earlier, we do not consider the diffusion of charged particles, which is characterized by diffusion frequency (Raizer 1991) $\nu_d = D/\Lambda^2$ where $D$ is the electron diffusion coefficient, and $\Lambda$ is a typical diffusion length. The case of glow discharge corresponds to the satisfaction of conditions $\nu_a > \nu_d$, $\nu_a > v_{dr}/L$, where $L$ is the distance between electrodes, and $v_{dr}$ is the drift velocity of charged particles. Estimations show that in air at atmospheric pressure, even at sufficiently low values of $E/N \approx 20$ Td, the diffusion length is approximately 2 km. Diffusion and gas-dynamic processes generate essentially more complex mathematical models described by multidimensional system of equations in partial derivatives, the analysis and solution of which is beyond the framework of the present chapter.

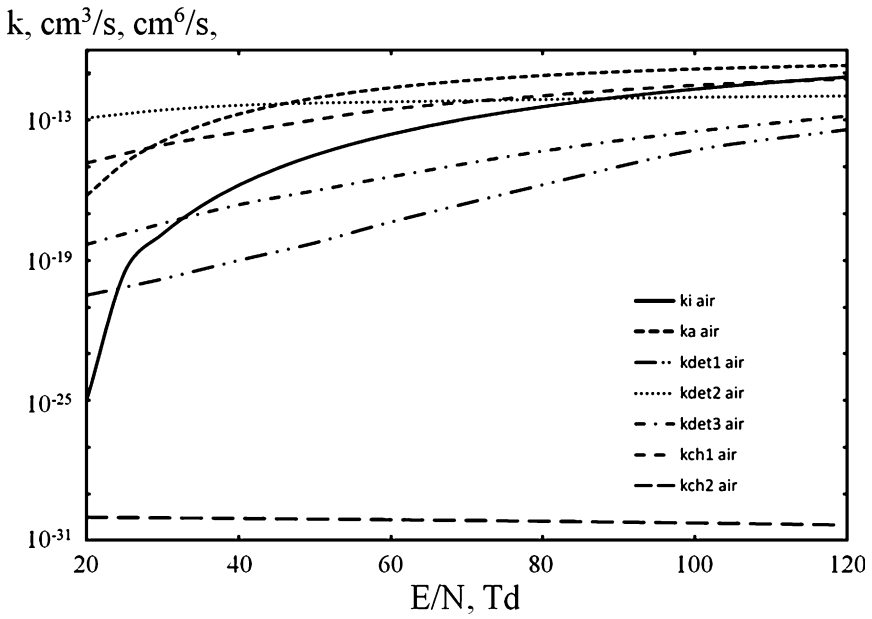


**Fig. 2.9** Rate constants of processes in air. — *ki* rate constant of air molecules ionization by electron impact (2.11), - - - *ka* rate constant of dissociative attachment of electrons to oxygen molecules (2.12), — ·· — *kdet1* rate constant of detachment in reaction (2.20), ····· *kdet2* rate constant of detachment in reaction (2.21), - · - *kdet3* rate constant of detachment in reaction (2.35), — *kch1* rate constant of charge-exchange reaction (2.36), — — *kch2* rate constant of ion-conversion reaction (2.37)

### Analysis of the Model Across Physical Parameters

We analyze the solution of the Cauchy problem for (2.38), (2.39), and (2.40) from the point of view of exponentially growing mode in the solution using concrete values of rate constants of the reactions depending on parameter *E*/*N* (electronic temperature).

Rate constants of reactions (2.20), (2.21), and (2.35) strongly depend on ion energies (Mnatsakanyan and Naidis 1991), which were accounted by us in the analysis. Rate constants of direct ionization $k_i$ (2.11) and dissociative attachment $k_a$ (2.12) in a constant electric field were calculated with the help of the Boltzmann equation's solution (see previous text) for the condition of glow discharge in the air. Charge-exchange (2.36) reaction rate constant $k_{ch1}$ was taken from (Smirnov 1974; Mnatsakanyan and Naidis 1991), and the rate constant of the ion-conversion reaction $k_{ch2}$ was taken from (Mnatsakanyan and Naidis 1991). Dependence of rate constant over *E*/*N* in the processes considered in the model is shown in Fig. 2.9.

The consequence of (2.38)–(2.40) is the third-order ordinary differential equation for concentrations of the plasma components as follows:

$$\frac{\mathrm{d}^3 y}{\mathrm{d}t^3} + a\frac{\mathrm{d}^2 y}{\mathrm{d}t^2} + b\frac{\mathrm{d}y}{\mathrm{d}t} + cy = q_y Q,$$
$$a = \nu_{\mathrm{det1}} + \nu_{\mathrm{det2}} + \nu_{\mathrm{det3}} + \nu_{\mathrm{ch1}} + \nu_{\mathrm{ch2}} + \nu_a - \nu_i,$$
$$b = \nu_a(\nu_{\mathrm{det3}} + \nu_{\mathrm{ch1}} + \nu_{\mathrm{ch2}}) + \nu_{\mathrm{det3}}(\nu_{\mathrm{det1}} + \nu_{\mathrm{det2}} + \nu_{\mathrm{ch1}} + \nu_{\mathrm{ch2}}) - \nu_i(\nu_{\mathrm{det1}} + \nu_{\mathrm{det2}} + \nu_{\mathrm{det3}} + \nu_{\mathrm{ch1}} + \nu_{\mathrm{ch2}}),$$
$$c = -\nu_{\mathrm{det3}}(\nu_i(\nu_{\mathrm{det1}} + \nu_{\mathrm{det2}} + \nu_{\mathrm{ch1}} + \nu_{\mathrm{ch2}}) - \nu_a\nu_{\mathrm{ch2}}),$$

where $y = \{\mathrm{N}_e, \mathrm{N}_{\mathrm{O}^-}, \mathrm{N}_{\mathrm{O}_2^-}\}$ is any of the quantities specified in brackets, and the right parts are positive and various at different $y$ as follows:

$$q_e = \nu_{\mathrm{det3}}(\nu_{\mathrm{det1}} + \nu_{\mathrm{det2}} + \nu_{\mathrm{ch1}} + \nu_{\mathrm{ch2}}), \quad q_{\mathrm{O}^-} = \nu_{\mathrm{det3}}\nu_a, \quad q_{\mathrm{O}_2^-} = \nu_a\nu_{\mathrm{ch1}}.$$

At condition $c \neq 0$, which we consider to be fulfilled in further analysis, a general solution of this equation looks like this:

$$y = C_{y1}\exp(\lambda_1 t) + C_{y2}\exp(\lambda_2 t) + C_{y3}\exp(\lambda_3 t) + \frac{q_y}{c}Q, \tag{2.41}$$

where $\lambda_1, \lambda_2, \lambda_3$ are roots of the characteristic equation:

$$p_3(\lambda) \equiv \lambda^3 + a\lambda^2 + b\lambda + c = 0 \tag{2.42}$$

Finally, depending on parameters $N$, $E/N$, constants $C_{y1}, C_{y2}, C_{y3}$ in (2.41) are various at different $y$, and they are determined with the help of initial data. The general solution (2.41) is constructed with use of the particular solution $y = \frac{q_y}{c}Q$ of the inhomogeneous equation.

Roots of the characteristic equation (2.42) define a character of solution (2.41); in particular, the presence of positive root causes the exponentially growing mode in the solution, which we interpret as ionization avalanche. Therefore, we further undertake the analysis of roots of the characteristic equation (2.42) for conditions 20 Td $< E/N <$ 120 Td and for concentration $N$ in air corresponding to altitudes $h \leq 100$ km. Let us formulate statements about the roots of (2.42), and then we will give short explanations proving such statements.

1. At condition $c < 0 (> 0)$, (2.42) has a positive (negative) real root $\lambda_1 > 0 (< 0)$.
2. In the considered range of $E/N$ and $h$ parameters, all three roots of (2.42) are real.
3. At condition $c < 0$ in the considered range of $E/N$ and $h$ parameters, (2.42) has one positive and two negative roots. This statement guarantees the absence of other exponentially growing modes except for the first one ($\lambda_1 > 0$).
4. At condition $c > 0$ in the considered range of $E/N$ and $h$ parameters, all three roots of (2.41) are negative. This statement guarantees the absence of exponentially growing modes at $c > 0$; because of this it is possible to consider that in

(2.38), (2.39), and (2.40), condition $c = 0$ gives a threshold of ionization avalanche, and condition $c < 0$ determines the breakdown values of $E/N$ and $h$ parameters.

The validity of statement no. 1 follows from the graph of cubic parabola $p_3(\lambda)$ (see (2.42)), which at $p_3(0) = c < 0 (> 0)$ crosses the positive (negative) part of abscissa at the point corresponding to the positive (negative) root of (2.42).

To proving the other statements, we use known properties of roots $\lambda_1, \lambda_2, \lambda_3$ of cubic equation (2.42) (Korn and Korn 1968) as follows:

(a) The type of roots is defined by the discriminant:

$$\Delta = -4a^3c + a^2b^2 - 4b^3 + 18abc - 27c^2.$$

At condition $\Delta > 0$, all roots are real.

(b) The roots of (2.42) are connected with its coefficients by the following relationships:

$$\lambda_1 + \lambda_2 + \lambda_3 = -a, \quad \lambda_1\lambda_2 + \lambda_1\lambda_3 + \lambda_2\lambda_3 = b, \quad \lambda_1\lambda_2\lambda_3 = -c. \tag{2.43}$$

From property (a) follows statement 2 at condition $\Delta > 0$. The latter is checked graphically in the considered range of parameters by an image of the level lines of function $\Delta(E/N, N)$.

Hereafter we use graphs to analyze root properties defined by the coefficients of (2.42). Obtaining the usual formula is practically impossible by virtue of root-formula complexity and also by virtue of the fact that the dependences of reaction-rate constants on $E/N$ are set initially by tables, and interpolation of these tables is used here.

Let us consider statement no. 3 (the case $c < 0$). Here, $\lambda_1 > 0$ accords with statement no. 1. From the third equality in (2.43) and the positivity of $\lambda_1$, it follows that $\lambda_2\lambda_3 > 0$ and roots $\lambda_2, \lambda_3$ are of the same sign. It can be determined graphically that $a > 0$ in the considered range of the parameters and then from the first (2.43) equality follows $\lambda_2 + \lambda_3 < 0$; hence, both roots $\lambda_2, \lambda_3$ are negative.

Let us consider statement no. 4 (the case $c > 0$). Here, $\lambda_1 < 0$ accords with statement no. 1. From the third equality in (2.43) and the negativity of $\lambda_1$, it also follows that $\lambda_2\lambda_3 > 0$ and roots $\lambda_2, \lambda_3$ are of the same sign. Graphically, from the image of lines $c = 0, b = 0$ in the plane of variables $E/N, N$ , it is shown that $b > 0$ at $c > 0$ in the considered range of these parameters.

Let us transform the second equality from (2.43) using the first one:

$$\begin{aligned} 0 < b &= \lambda_1(\lambda_2 + \lambda_3) + \lambda_2\lambda_3 = -(\lambda_2 + \lambda_3 + a)(\lambda_2 + \lambda_3) + \lambda_2\lambda_3 \\ &= -(\lambda_2 + \lambda_3)^2 - a(\lambda_2 + \lambda_3) + \lambda_2\lambda_3 \\ &= -\lambda_2^2 - \lambda_3^2 - \lambda_2\lambda_3 - a(\lambda_2 + \lambda_3) \Rightarrow \lambda_2 + \lambda_3 < 0. \end{aligned}$$

From this algebraic formula, it follows that the negativity of $\lambda_2, \lambda_3$ values is true by virtue of the positivity of $a, \lambda_2\lambda_3$ values.

From the positivity of the solution to the Cauchy problem for (2.38), (2.39), and (2.40), it follows that $C_{1y} > 0$ in (2.41) at condition $c < 0$; otherwise, the solution becomes negative at high time values (in the long term) due to an infinite increase of the first exponent in (2.41). Direct analysis of the positivity of solution (2.41) at any non-negative initial data is sufficiently complex. We have proven that $C_{1e} > 0$ at zero initial data for (2.38), (2.39), and (2.40), in addition, positivity of the solution is confirmed under different conditions by numeric solution of the Cauchy problem for this system.

Thus, at condition $c < 0$ in the considering model there exists only one exponentially growing mode ($\lambda_1 > 0$), which is interpreted as a physical ionization avalanche.

Condition $c < 0$ in the explicit form looks like this:

$$\nu_i(\nu_{\text{det1}} + \nu_{\text{det2}} + \nu_{\text{ch2}} + \nu_{\text{ch1}}) - \nu_a\nu_{\text{ch2}} > 0$$

or this:

$$k_i > \frac{k_a k_{\text{ch2}} \eta_{O_2}^3}{\left(k_{\text{det1}} + k_{\text{det2}}\eta_{N_2} + k_{\text{ch1}}\eta_{O_2} + k_{\text{ch2}} N \eta_{O_2}^2\right)} N, \tag{2.44}$$

where $\eta_{M_2} = \eta_{M_2}/\eta$ is a proportion of molecules $M_2$ in the composition of the air.

It follows from (2.44) that in the given model, the presence of the threshold is defined by constants $k_a, k_{\text{ch2}}$ of dissociative attachment (2.12) and three-body conversion (2.37) of ion $O^-$ into $O_3{}^-$. In case of the absence of one of these processes ($k_a k_{\text{ch2}} = 0$), condition (2.44) is always satisfied, and there is no threshold as in the previous model (2.26), (2.27). Breakdown condition (2.44) depends on gas concentration $N$ (over the altitude), which is conditioned by three-body reaction (2.37). One must note the qualitative similarity of breakdown conditions for the simplest model (2.13) of direct ionization-dissociative attachment and those of the more complex models (2.38), (2.39), and (2.40), which are written as $k_i > \beta k_a$ with different coefficients $\beta$. In (2.13) $\beta = \eta_{O_2}$and in (2.38), (2.39), and (2.40), $\beta$ depends on gas concentration and on parameter $E/N$ through the rate constants of reactions of secondary electron appearance (detachment) and elimination of main negative ion $O^-$.

With increased altitude, concentration N decreases, and the term $k_{\text{ch2}} N \eta_{O_2}^2$ decreases in the denominator of (2.44). Estimations performed with accounting of the rate-constant dependence on pressure (altitude) show that at $h > 40$ km, the term $k_{\text{ch2}} N \eta_{O_2}^2$ in the denominator of (2.44) becomes insignificant, and the inequality in (2.44) looks like this:

$$k_i > \frac{k_a k_{\text{ch2}} \eta_{O_2}^3}{\left(k_{\text{det1}} + k_{\text{det2}}\eta_{N_2} + k_{\text{ch1}}\eta_{O_2}\right)} N.$$

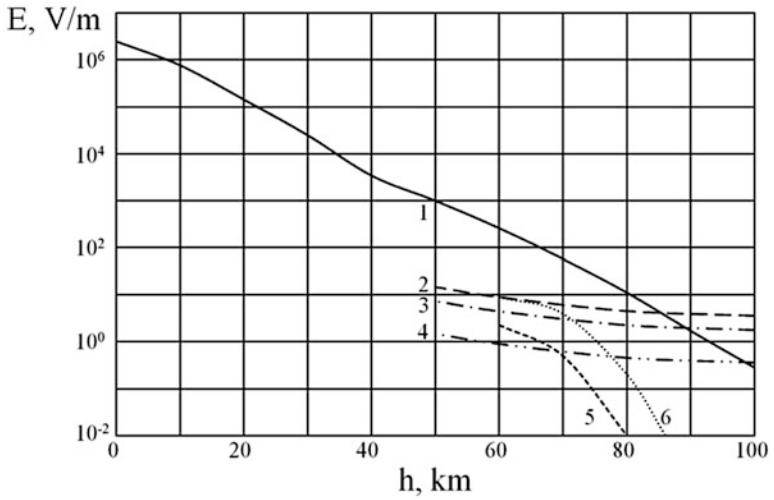


**Fig. 2.10** Comparison of breakdown electric field dependence on altitude (2.44) with experimentally measured electric fields in the mesosphere and theoretical electric fields of cloud charges. *1* (2.44); electric fields created by cloud charges (located at altitude 5 km) of values *2* 10 C, *3* 5 C, and *4* 1 C, respectively; *5* and *6* electric fields registered at altitudes 60–90 km (Zadorozhny and Tyutin 1998)

To determinate the threshold field at which ionization avalanche begins, one must base it on the inequality in (2.44) to determine the smallest value of parameter *E*/*N* at which it is satisfied while taking into account the dependences of *E*/*N* of the frequencies of the processes entering into (2.44). A dependence of neutral concentration over height was taken from the standard atmosphere model (Sedunov 1991; Brasseur and Solomon 1984).

In Fig. 2.10 one can see the dependences of the threshold electric field obtained on the basis of (2.44). In the same figure are represented the dependences over altitude of electric fields created by a 5-km cloud charge at values of 10 C , 5 C , and 1 C, respectively. Calculations were carried out with a help of the following formula (Raizer et al. 1998):

$$E \equiv E(h) = \frac{z \cdot Q}{\pi \cdot \varepsilon_0 h^3}\left[1 + \left(\frac{h}{2 \cdot h_i - h}\right)^3\right], \tag{2.45}$$

where $z$ is the altitude of the cloud location, $Q$ is a value of the cloud charge, $h$ is the point of $E(h)$ determination over the earth, and $h_i$ is the altitude of the ionospheric location over the earth.

In Fig. 2.10, one can also see the experimental data on electric fields measured at the mesosphere level from (Zadorozhny and Tyutin 1998). As is well known (Sedunov 1991), the atmospheric electric field changes from a typical value of

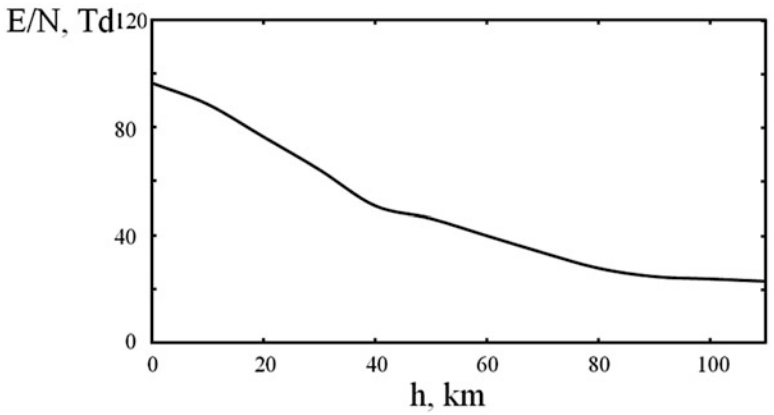


**Fig. 2.11** Dependence of threshold-reduced electric field (2.44) on altitude (Ardelyan et al. 2012b, 2013b)

130 V/m in fair weather (3,000 V/m during thunder storms) at the ground level and to practically zero at an altitude of approximately 4 km (Sedunov 1991). Its low values allows one to disregard it in models of ionization processes realized by different discharges with typical values of electric fields much greater than those of the background atmosphere.

From Fig. 2.10, one can see that the electric field of a charge 1C cloud reaches the value of the threshold field at an altitude of approximately 100 km; for a charge 5C cloud this altitude is approximately 90 km; and for a charge 10 C cloud this altitude is approximately of 85 km. From Fig. 2.10, one can see that fields of noncompensated charged clouds can lead to the breakdown of air at altitudes of 80–100 km, thus serving as ionizers for the development of high-altitude discharges in the mesosphere.

In Fig. 2.11, dependence of the threshold electric field on the altitude obtained by the inequality (2.44) is presented (Ardelyan et al. 2012b, 2013b). From this graph, one can see that with increased altitude, the value electric field threshold decreases. At greater altitudes, the speed of this decrease becomes less, and the threshold field is limited to $E/N \sim 25$ Td. Deceleration of threshold fields with altitude is defined by the decreased efficiency process in (2.37) (see previous text).

Our analysis shows that air breakdown depends on the time of discharge activity, parameter $E/N$, and altitude above the ground (concentration of neutrals and air temperature). The values of rate constants depend on the type of discharge and thus determine the values of $E/N$ parameter under concrete conditions (for example, values of threshold electric fields created by Radio Frequency (RF) discharges differ from those created by glow discharges) (Aleksandrov et al. 2008; Mnatsakanyan and Naidis 1991).

With increased altitude above the ground, the breakdown field in dry air decreases, and in the mesosphere it decreases considerably in connection with a significant decrease of oxygen molecule concentration.

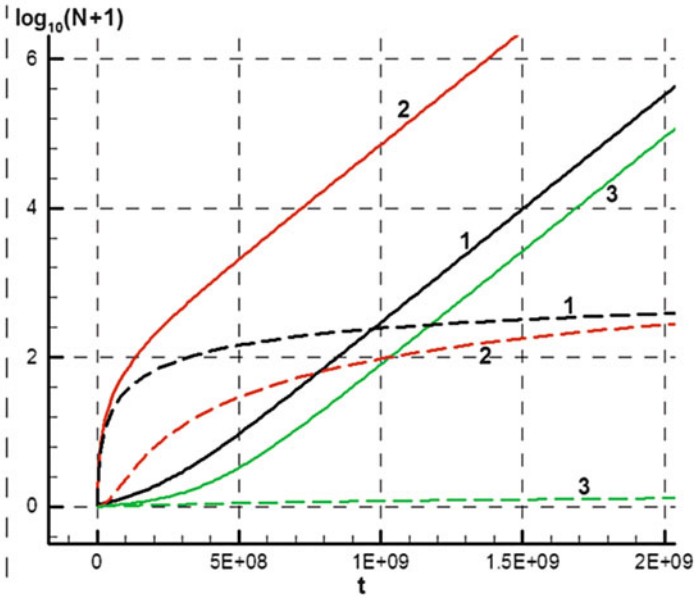


**Fig. 2.12** Numerical solution of the model problem at initial concentrations of components $10^{-6}$ cm$^{-3}$. Altitude $h = 70$ km, electric field strength value $E = 0.8$ V/cm (*solid lines*), and $E = 0.4$ V/cm (*dashed lines*). *1* $N_e$ (*black*), *2* $N_{O_2^-}$ (*red*), *3* $N_{O^-}$ (*green*). Scales over axes: $N$ cm$^{-3}$, $t$ μs

### Illustrative Examples

Let us consider illustrative examples of the application of (2.38), (2.39), and (2.40). Concrete variants of the model are defined by values of an electric field and the density of air (altitude above a surface of the Earth) or the parameters $E/N$, $h$. The modeling analysis is set at altitude $h = 70$ km ($N = 1.71 \cdot 1{,}015$ cm$^{-3}$) because concentrations of main components are such that all of stages can be considered within the same time scale.

At breakdown electric field $E = 0.8$ V/cm ($E/N \approx 46.8$ Td), when condition (2.44) is satisfied, the roots of the characteristic equation take the following values:

$$\lambda_1 \approx 7.03 \cdot 10^{-9} \ \mu s^{-1}, \quad \lambda_2 \approx -10^{-3} \ \mu s^{-1}, \quad \lambda_3 \approx -5.29 \cdot 10^{-6} \ \mu s^{-1}. \quad (2.46)$$

In correspondence with the above analysis, the first root is positive, and the two others are negative. At the stage of predominancing the exponentially growing mode $e^{\lambda_1 t}$, plasma concentration growth for an order of magnitude takes place during time $\Delta t = \ln 10/\lambda_1 \approx 0.33 \cdot 10^9$ μs.

Under breakdown field $E \approx 0.4$ V/cm ($E/N = 23$ Td), when condition (2.44) is not satisfied, then the roots of the characteristic equation take the negative values $\lambda_1 \approx -2.24 \cdot 10^{-4}$ μs$^{-1}$, $\lambda_2 \approx -1.25 \cdot 10^{-9}$ μs$^{-1}$, and $\lambda_3 \approx -3.32 \cdot 10^{-11}$ μs$^{-1}$.

In Fig. 2.12 one can see concentrations of the plasma components with respect to time for both indicated variants as obtained by a numerical solution of (2.38),

(2.39), and (2.40) at initial values of plasma components concentrations equal to $10^{-6}$ cm$^{-3}$.

Under breakdown field $E = 0.8$ V/cm, ion $O_2^-$ prevails, the concentrations of which at the developed stage exceed the concentration of electrons by two orders of magnitude, and "electro-negative plasma" is formed.

Under breakdown field $E = 0.4$ V/cm, the concentrations of plasma components tend to constant values different from zero; this is conditioned by the process of breakdown ionization (2.15) by fast particles. The latter agrees with the general solution (2.41) in which the exponential components tend to zero with time.

### Comparison with the Full Model

In terms of comparing the solution of (2.38), (2.39), and (2.40) with that of the "full model," the main results are presented in the Sect. 2.3. Developed and used by us, the full model of air plasma chemical kinetics (see Sect. 2.4) comprises 27 ordinary differential equations, 25 of which describe the balance of plasma components (ions, neutrals, excited molecules), and 2 of which are energy equations of the gas and the electrons. Here, for example, we also consider the altitude of 70 km because the concentrations of main components at this altitude are such that all stages can be considered within the same time scale.

In Fig. 2.13, one can see a comparison of numerical solutions to (2.38), (2.39), and (2.40) as well as that of the full model at initial values of a plasma component concentration equal to $10^{-6}$ cm$^{-3}$. Graphs of the plasma components participating in the linear model, as well as the temperature of the gas in the full model, are also presented.

At the indicated initial (small) values at the initial stage (the stage of the prebreakdown ionization) at $t < 6 \cdot 10^8$ μs, the linear model well approaches the solution of the full model. At this stage in the full model, the positively charged components of the plasma are presented by the ion $O_2^+$, and the gas temperature does not change. The comparison given indicates the physical adequacy of the linear model (2.38)–(2.40).

At the following nonlinear stage in the full model, further ionization takes place under another script. The electron concentration grows, and the plasma becomes electron-ion; this process is accompanied by the replacement of ion $O_2^+$ with ion $NO^+$ and growth of the gas temperature to ≥2,000 K. At this stage of discharge development, one can identify a stage of the breakdown, *i.e.*, strongly nonlinear ionization. Then there comes a stage after the breakdown of discharge development when the concentration of electrons varies weakly, but the concentrations and the composition of ions can vary, with the latter coming the post-breakdown stationary (or quasi-stationary) state.

This comparison does not mean that three-component linear models (2.38), (2.39), and (2.40) always adequately describe the prebreakdown ionization stage (see section. "Illustrative examples"). At other initial conditions, other scripts of

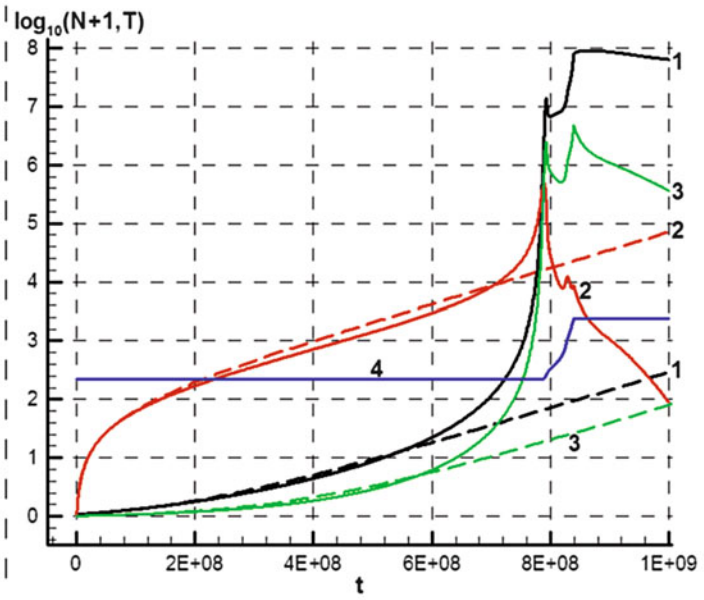


**Fig. 2.13** Numerical solution in the linear model (*dashed lines*) and the full model (*solid lines*) at initial concentrations of components $10^{-6}$ cm$^{-3}$. Altitude $h = 70$ km, and values of electric field strength $E = 0.8$ V/cm. *1* $N_e$ (*black*), *2* $N_{O_2^-}$ (*red*), *3* $N_{O^-}$ (*green*), *4* gas temperature $T$ (*dark blue*). Scales over axes: $N$ cm$^{-3}$, $t$ μs, $T$ K

prebreakdown ionization are possible, described by others, probably more complex models that require research. This statement is illustrated by Fig. 2.14, in which the calculation results of discharge over the full model are presented under the same physical parameters—$h = 70$ km, $E = 0.8$ V/cm—but at background initial conditions calculated for the power of fast-particle source $W = 18$ eV/(cm$^3$·s) (electron–ion pair production per unit of volume per unit of time $G = 0.57$ cm$^{-3}$·s$^{-1}$ at $h = 70$ km [Brasseur and Solomon 1984]). Background values of the plasma components are represented in the left part of the Fig. 2.14 where the initial stage of the prebreakdown ionization is presented at an increased scale over time.

Here as well as in Fig. 2.13, in the case of very small values of initial data, the linear initial stage of prebreakdown ionization at $t < 3 \cdot 10^7$ μs is observed. In this stage, concentrations of the plasma components grow exponentially (linearly in the logarithmic scale in Fig. 2.14). The script (the linear model) differs from the one examined here, and one can see that the growth rate in this case is substantially greater than that in the model (2.38)–(2.40) as well as that of the full model in Fig. 2.13. The stage of breakdown ionization ($6{\cdot}10^7$ μs $< t < 9{\cdot}10^7$ μs) takes place with a sufficiently fast increase of temperature. One can see an intermediate stage between the stages of prebreakdown and breakdown ionization ($3{\cdot}10^7$ μs $< t < 6{\cdot}10^7$ μs), in which the temperature increased more slowly and the electron concentration almost does not vary. The intermediate stage with slowly

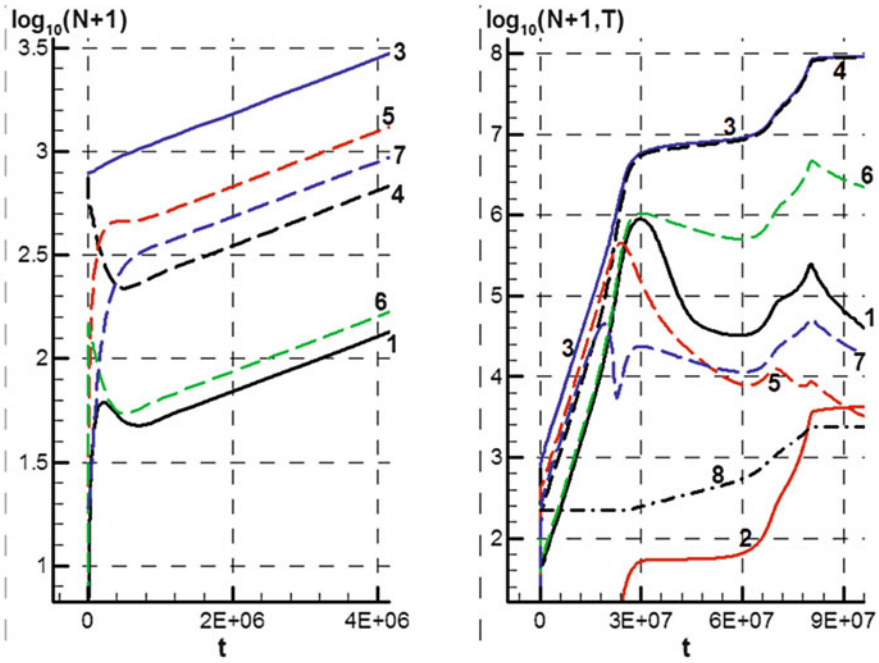


**Fig. 2.14** Numerical solution of the full model at the given background concentrations. Altitude $h = 70$ km, and electric field strength $E = 0.8$ V/cm. *1* $N_{O_2^+}$, *2* $N_{N_2^+}$, *3* $N_{NO^+}$, *4* $N_e$, *5* $N_{O_2^-}$, *6* $N_{O^-}$, *7* $N_{O_3^-}$, and *8* gas temperature $T$. Scales over axes: $N$ cm$^{-3}$, $t$ μs, $T$ K

changing (and even decreasing) electron concentration, one can see in Fig. 2.13 ($t \sim 8 \cdot 10^8$ μs) and this takes approximately the same time as that shown in Fig. 2.14.

The results of calculations presented in Figs. 2.13 and 2.14 show that the script and time of breakdown development can depend strongly on initial conditions. At initial conditions close to zero, this time is almost an order of magnitude greater than that at background (nonzero) initial conditions.

Within the limits of the linear model (2.38)–(2.40), it is impossible to determine the time characteristics of the ionized area coming to near breakdown and post-breakdown modes when it cannot be limited in the prebreakdown stages by a simple linear plasma chemical model that does not consider ion-ion and ion-molecular processes as well as those describing excited particles in the air at their origination by external sources of excitation. Therefore, the results obtained play an auxiliary role allowing to reasonably estimate a threshold field and choose key parameters in a detailed quantitative analysis on the basis of more complex models and, by this, to decrease the number of parameters in time-consuming calculations. The following part of this chapter is devoted to the numerical modeling of electric breakdown in the atmosphere on the basis of the full model.

## 2.4 Numerical Analysis of Breakdown Phenomena in Air

In this section, we consider plasma chemical processes at near-breakdown values of electric field in dry air at altitudes of 0–90 km. We undertake calculations of concentrations of the main charged particles, electron and gas temperatures at the gas-discharge excitation of air.

### *2.4.1 Model*

As in our previous works (Ardelyan et al. 2001, 2012a, 2013a), for initial analysis of the plasma-chemistry of dry air, we chose the full model of chemical kinetics. The system of plasma chemical reactions corresponds to works (Ardelyan et al. 2013a; Kossyi et al. 1992), which represents 27 ordinary differential equations, 25 of which describe the balance of plasma components (ions, neutrals, excited molecules) and 2 of which are equations of gas and electron energy as well as 180 plasma chemical reactions. The EFDE was considered corresponding to the glow discharge (see Sect. 2.2), and, with the help of this, the main rate constants of electron molecule reactions were obtained. Determination of the influence of fast particles on the background and the corresponding costs of molecule excitation, dissociation, and ionization was taken from (Ardelyan et al. 2013a; Maetzing 1991).

As indicated previously, the equations contained that of electron temperature in the form of (Zadorozhny and Tyutin 1998; Ardelyan et al. 2001, 2012a, 2013a). These works described the following: (1) the heating of electrons in an external electric field; (2) the heating of plasma electrons at the injection of fast electrons into the area below the threshold of vibrational excitation (Ardelyan et al. 2013a; Konovalov and Son Konovalov and Son 1987); (3) the heating of plasma electrons in processes of electron-ion recombination (Ardelyan et al. 2013a; Konovalov and Son 1987); (4) the heating of plasma electrons in processes of electron detachment from negative ions; (5) the cooling of plasma electrons in the process of electron attachment to molecule $O_2$ (Bychkov and Eletskii 1985); and (6) the heating of plasma electrons in elastic and inelastic collisions with molecules $O_2$ and $N_2$.

In the equation for gas temperature $T$, we included summands corresponding to gas heating resulting from the relaxation of electronic and vibrationally levels of freedom (Ardelyan et al. 2013a), the heating and cooling of the gas in chemical and plasma chemical reactions, and Joule heating (heating by electrons in collisions). In modeling, we described reactions with the participation of positive ions $O^+$, $O_2^+$, $O_4^+$, $O_6^+$, $O_8^+$, $N^+$, $NO^+$, and $N_2^+$; negative ions $O^-$, $O_2^-$, and $O_3^-$; atoms N and O; molecules $O_2$, $O_3$, $N_2$, $N_2O$, and NO; vibrationally excited states of nitrogen $N_2(v)$; electronically excited states of nitrogen $N_2(b)$ and $N_2(z)$; vibrationally excited states of oxygen $O_2(v)$; and electronically excited states of oxygen $O_2(^1\Delta_g)$ (see details in Ardelyan et al. 2013a). We described recombination reactions of each positive ion

with each negative ion. Data of these processes were determined on a basis of the Flannery approach (Smirnov 1974; Kossyi et al. 1992; Smith and Thomson 1978) in describing temperature and pressure (Ardelyan et al. 2013a). In the calculations, we supposed that de-excitation of the vibrational and rotational states of molecules takes place mainly at collisions with molecules. The model also includes charge-exchange reactions of ions (Ardelyan et al. 2013a; Smith and Thomson 1978; Virin et al. 1979). The power inputted to the gas by fast particles W is defined in units of eV/($cm^3$·s), and the rate of excitation $Q$ is usually connected with this by $Q = W/(U_i)$ (Ardelyan et al. 2012a, 2013a), where $U_i$ is the cost of the ionization, in particular, in air $U_i = 31.6$ eV. The calculations were carried out under an approximation of constant density where the model used represents the ordinary differential equations. More details about the code, tables of plasma chemical processes, rate constants, and the model of air plasmas can be found in (Ardelyan et al. 2013a).

In the analysis, we first determined background values of the components similar to those described in section "Comparison with the full model", but a full set of components at the given values of the excitation and ionization costs depends on the altitude and temperature recorded (Sedunov 1991; Brasseur and Solomon 1984). These served as initial values for chemical kinetic calculations of charged, neutral, and excited particles in the plasma. This corresponded to the modeling of an established plasma chemical balance at the given altitude at the given pressure and temperature.

At all altitudes, values of $E/N$ parameters were selected so that the breakdown took place during approximately 100 s; this corresponds to the discharge time of the unipolarly charged macro object in the atmosphere (Bychkov et al. 2010).

### 2.4.2 Results of Calculations

#### General Results

In Figs. 2.15, 2.16, 2.17, 2.18, and 2.19, the results of calculations of the main ions, electrons, and gas temperatures for the discharge in air are presented for different altitudes above the ground and for different values of external electric field strength. Dependence of the temperature on time is represented at different values of the electric field; these show how the field influences the kinetics of gas warming, thus promoting improved ionization.

In Fig. 2.15 one can see the results of calculations of main ions, electrons, and gas temperature at $h = 0$ km, $E = 14.5$ kV/cm and a value of parameter $E/N = 57$ Td. At the initial stage of field influence on air at time $t \leq 20$ s, the generation of negative ions due to electron attachment to oxygen molecules and the following ion transformation takes place. The balance of negatively and positively charged particles is realized by ions $O_3^-$, $O_2^-$, and $NO^+$. At time approximately $t \sim 140$ *s*, heating of the gas from $T = 282$ K to $T = 2{,}240$ K occurs. At the latter temperature, effective detachment of electrons from negative ions takes place, and their balance

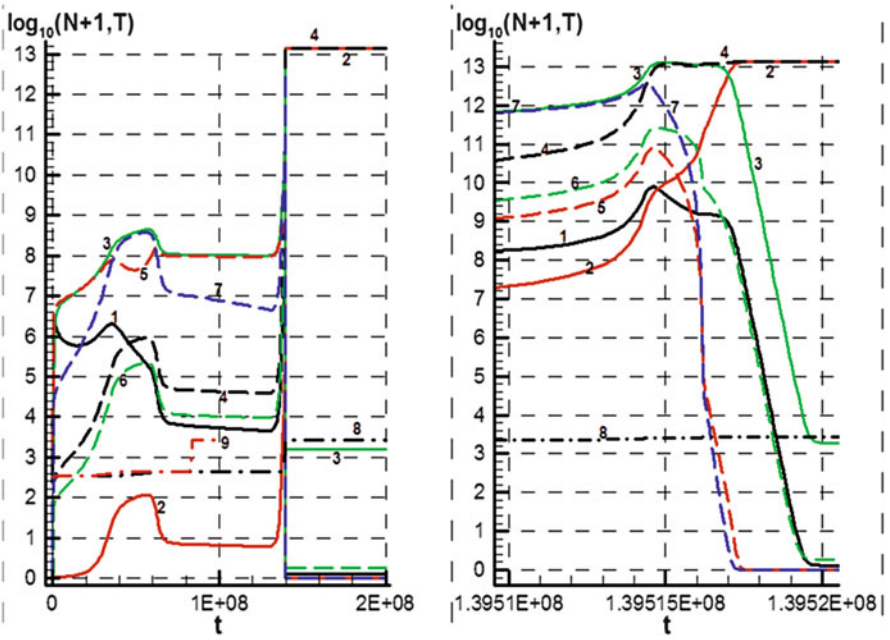


**Fig. 2.15** Concentrations of main ions, electrons. and gas temperature at $h = 0$ km, $E = 14.5$ kV/cm. *1* $O_2^+$, *2* $N_2^+$, *3* $NO^+$, *4* e, *5* $O_2^-$, *6* $O^-$, *7* $O_3^-$, *8 T* (*black dash* pointed line at $E = 14.5$ KB/cm; and *9* T (*red pointed line* $E = 15$ kV/cm). *N* $cm^{-3}$, *t* μs, *T* K. Figures correspond to different time scales

is realized mainly by ions $NO^+$. In this case, the avalanche's strongly nonlinear increase of electron concentration takes place, and one can consider the occurrence of gas breakdown. At $E = 15$ kV/cm and initial parameter $E/N = 59$ Td, gas heating takes place during $t \sim 20$ s, and the electric gas breakdown occurs earlier.

In Fig. 2.16, one can see the results of calculations of main ions, electrons, and gas temperature at $h = 5$ km, $E = 8.7$ kV/cm as well as value of parameter $E/N = 57$ Td. At the initial stage of field influence on air at time $t \leq 40$ s, generation of negative ions takes place. The balance of negatively and positively charged particles is realized by ions $O_3^-$, $O_2^-$, and $NO^+$. At time, $t \sim 160$ s, gas heating to temperature $T = 2{,}240$ K occurs, and the balance of the charged particles is realized mainly by electrons and $NO^+$. In this case, the strongly nonlinear stage of gas breakdown takes place. At $E = 9$ kV/cm and the initial value of parameter $E/N = 59$ Td, gas heating leads to the breakdown threshold shifting to $t \sim 20$ *s*.

In Fig. 2.17 one can see the results of calculations of main ions, electron, and gas temperature at $h = 30$ km, $E = 165$ V/cm as well as the value of parameter $E/N = 43$ Td. At the initial stage of field influence on air at time $t \leq 90$ s, generation of negative ions takes place. The balance of negatively and positively charged particles is realized by ions $O_2^-$ and $NO^+$. At time $t \sim 155$ *s*, gas heating to $T = 2{,}500$ K occurs, and the balance of the charged particles is realized mainly

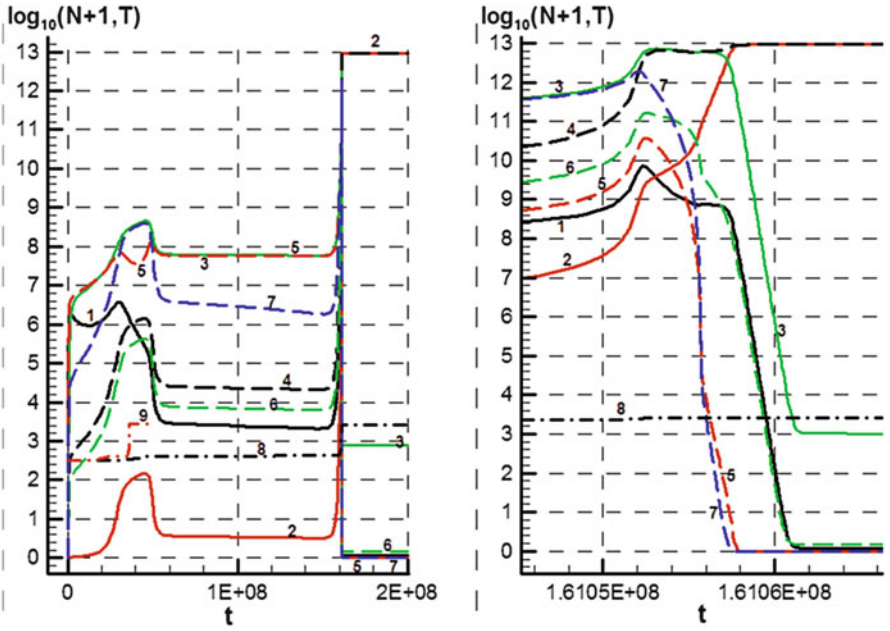


**Fig. 2.16** Concentrations of main ions, electrons, and gas temperature at $h = 5$ km, $E = 8.7$ kV/cm. *1* $O_2^+$, *2* $N_2^+$, *3* $NO^+$, *4* e, *5* $O_2^-$, *6* $O^-$, *7* $O_3^-$, *8* T (*black dashed line* $E = 8.7$ kV/cm), and *9* T (*red dashed line* $E = 8.9$ kV/cm). $N$ cm$^{-3}$, $t$ μs, $T$ K. Figures correspond to different time scales

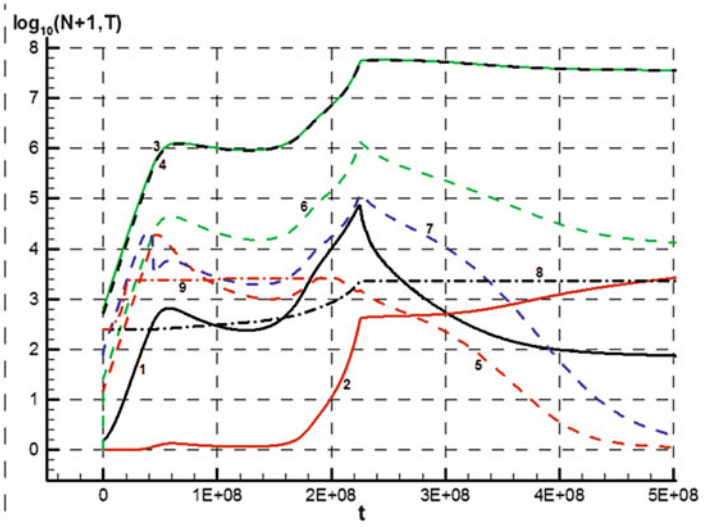


**Fig. 2.17** Concentrations of main ions, electrons, and gas temperature at $h = 30$ km, $E = 165$ V/cm. *1* $O_2^+$, *2* $N_2^+$, *3* $NO^+$, *4* e, *5* $O_2^-$, *6* $O^-$, *7* $O_3^-$, *8* T (*black dashed line* $E = 165$ V/cm), and *9* T (*red dashed line* $E = 180$ V/cm). $N$ cm$^{-3}$, $t$ μs, $T$ K. Figures correspond to different time scales

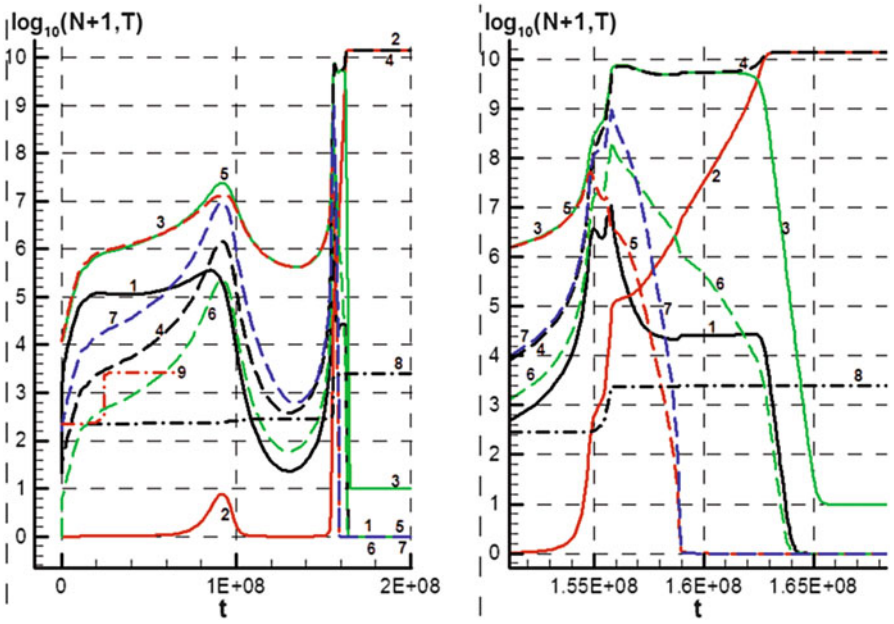


**Fig. 2.18** Concentrations of main ions, electrons, and gas temperature at $h = 60$ km, $E = 2.5$ V/cm. *1* $O_2^+$, *2* $N_2^+$, *3* $NO^+$, *4* e, *5* $O_2^-$, *6* $O^-$ *7* $O_3^-$, *8* T (*black dashed line* $E = 2.5$ V/cm), and *9* T (*red dashed line* $E = 3.0$ V/cm). $N$ cm$^{-3}$, $t$ μs, $T$ K

by electrons and ions $NO^+$. In this case, the strongly nonlinear stage of gas breakdown takes place. At $E = 180$ V/cm and an initial value of parameter $E/N = 47$ Td, gas heating leads to the breakdown threshold shifting to $t \sim 20$ *s*.

In Fig. 2.18, one can see results of calculations of main ions, electrons, and gas temperature at $h = 60$ km, $E = 2.5$ V/cm, as well as the value of parameter $E/N = 39$ Td. Because the concentration of $O_2$ increases with increasing altitude, then the origination of ions $O_2^-$ in reaction (2.18) quadratic over $O_2$ decreases sharply. In this case, the balance of charged particles is realized by electrons and ions $NO^+$ practically from the beginning of discharge activity. Processes are similar to those considered in the third section in the model for three ions. Warming leads to additional growth of the electron concentration because the temperature growth decreases electron-ion recombination. The increase of the applied field stimulates the breakdown phenomena even more strongly. In general, the picture of the breakdown occurring at altitudes of 60–90 km is the same and is similar to those considered by us in section "Comparison with the full model".

In Fig. 2.19, one can see the results of calculations of main ions, electrons, and gas temperature at $h = 90$ km, $E = 0.045$ V/cm, as well as the corresponding value of parameter $E/N = 64$ Td. This value of the $E/N$ parameter is approximately 2 times greater than those considered at altitude $h = 60$ km. Therefore, ion $O^-$ plays an important role in the formation of negative ions in (2.12) and their

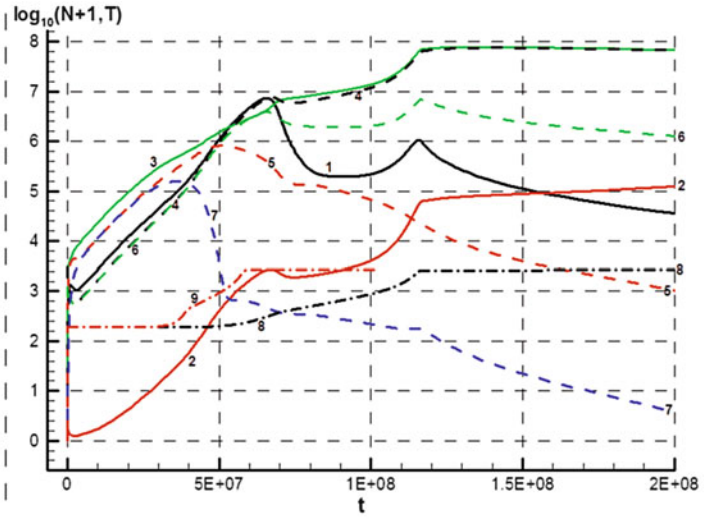


**Fig. 2.19** Concentrations of main ions, electrons, and gas temperature at $h = 90$ km, $E = 0.045$ V/cm. *1* $O_2^+$, *2* $N_2^+$, *3* $NO^+$, *4* e, *5* $O_2^-$, *6* $O^-$, *7* $O_3^-$, *8* T (*black dashed line* $E = 0.045$ V/cm), and *9* T (*red dashed line* $E = 0.05$ V/cm). $N$ cm$^{-3}$, $t$ μs, $T$ K

subsequent transformation to $O_3^-$. A small heating of gas is sufficient to destroy negative ions and realize air breakdown at times of approximately 60 s.

### Role of the Background State

Initial data for variants of fulfilled calculations are listed in Table 2.1. In this table, the number of the computed variant is indicated in the first column. The altitude for which the calculation is executed is indicated in the second column. The third column lists the concentration of neutrals at the given altitude, which was taken from the *Standard Atmosphere of USA* (Brasseur and Solomon 1984). Data on the velocity of fast-particle appearance $W$ with respect to altitude were taken from (Sedunov 1991; Brasseur and Solomon 1984; Wahlin 1994) and are listed in the fourth column.

Data from Sedunov (1991) and Wahlin (1994) agree at low altitudes and differ at altitude 4 km. At altitudes between 10 and 50 km, we used data extrapolated from Wahlin (1994). At low altitudes, the differences in data weakly influence the discharge parameters.

Along with values of the velocity of fast particles, we present in the same column a decreased velocity $W/N$ per one particle, which increases with increasing altitude. In the last column, the prevailing component concentration values in background plasma are presented. These were used as the initial data at numerical modeling of the discharge by the full model. These values were obtained by numerical solution with zero initial data, and the electric field and velocity of fast-particle appearance

**Table 2.1** Initial parameters for calculations (background plasma parameters)

| N. | $h$, km | $N$, $cm^{-3}$ | $W$, eV/($cm^3$s) ($W/N$, eV/s) | $E$, V/cm ($E/N$, Td) | Background component concentrations: $N$ – $cm^{-3}$; quasi- stationary time $t$ – s. |
|---|---|---|---|---|---|
| **1** | **0** | $2.55 \cdot 10^{19}$ | $3.7 \cdot 10^2$ (Sedunov 1991; Brasseur and Solomon 1984) ($1.44 \cdot 10^{-17}$) | $14.5 \cdot 10^3$, (56.8) $15 \cdot 10^3$, (58.8) | $N_{NO^+} \approx N_{O_2^-} \approx 10^3$, $N_{NO} \approx N_{O_3} \approx 10^7$, $t = 4 \cdot 10^5$ |
| **2** | **10** | $8.61 \cdot 10^{18}$ | $1.2 \cdot 10^3$ (Wahlin 1994) ($1.39 \cdot 10^{-16}$) | $4.75 \cdot 10^3$, (55.2), $5 \cdot 10^3$, (58.1), | $N_{NO^+} \approx 6.6 \cdot 10^2$; $N_{O_2^+} \approx 1.4 \cdot 10^3$; $N_{O_2^+} \approx 1.4 \cdot 10^3$; $O_6^+, O_8^+$ – are also present $N_{NO} \approx N_{O_3} \approx 10^7$, $t = 10^5$ |
| **3** | **30** | $3.83 \cdot 10^{17}$ | $2.9 \cdot 10^3$ (Wahlin 1994) ($7.57 \cdot 10^{-15}$) | 165, (43.1), 180 (45) | $N_{NO^+} \approx N_{O_2^-} \approx 10^4$, $N_{NO} \approx N_{O_3} \approx 10^{10}$, $t = 10^6$ |
| **4** | **60** | $6.45 \cdot 10^{15}$ | 11 (Brasseur and Solomon 1984) ($1.71 \cdot 10^{-15}$) | 2.5, (38.8), 3, (46.5) | $N_{NO^+} \approx N_e \approx 6.0 \cdot 10^2$, $N_{NO} \approx N_{O_3} \approx 10^{11}$, $t = 10^7$ |
| **5** | **90** | $6.98 \cdot 10^{13}$ | 290 (Brasseur and Solomon 1984) ($4.15 \cdot 10^{-12}$) | 0.045, (64.5), 0.05, (71.6) | $N_{NO^+} \approx N_e \approx 3.0 \cdot 10^3$, $N_{NO} \approx N_{O_3} \approx N_O \approx 10^9$, $t = 10^6$ |

are indicated in the fourth column of Table 2.1. The background quasi-stationary state is usually established during time $t =$ approximately $10^6$ s, which exceeds the typical time of external conditions (day to night) as they change in the atmosphere; therefore, the background values obtained have a qualitative character, specifying probable composition, and a concentration of the background plasma. For low altitudes (*i.e.*, variants no. 1 through no. 3) at times specified in Table 2.1, ions $NO^+, O_2^-$ prevail in background plasma; at high altitudes (*i.e.*, variants no. 4 and no. 5), electrons and ion $NO^+$, and at smaller time values than indicated in the table ions $O_2^+, O_2^-$ (variant 2), prevail in background plasma.

At high altitudes, the exit to a stationary state, with a prevalence of electrons and ions $NO^+$, takes place more quickly. The indicated stationary state is apparently final for any altitude; however, at low altitudes, the exit to a stationary state at times essentially exceeds the time when atmospheric conditions change. The general idea of dependence of the background solution on time is shown in Fig. 2.20, which presents concentrations of the background plasma's main charged components at altitude 60 km (variant 4) in a logarithmic scale over time.

For other variants in Table 2.1, the qualitative picture of Fig. 2.20 does not change. It elongates over time with decreased altitude (increased density); the numerical values of concentrations depend on air density $N$ and decreased velocity of fast-particle ionization $W/N$ per one particle.

For all altitudes, typically there is the presence of a significant amount of neutral $NO, O^3, O$ in low-ionized plasmas. This essentially influences the beginning of prebreakdown ionization when the electric field is switched on. The degree of ionization of background plasma increases with altitude due to reduction of air

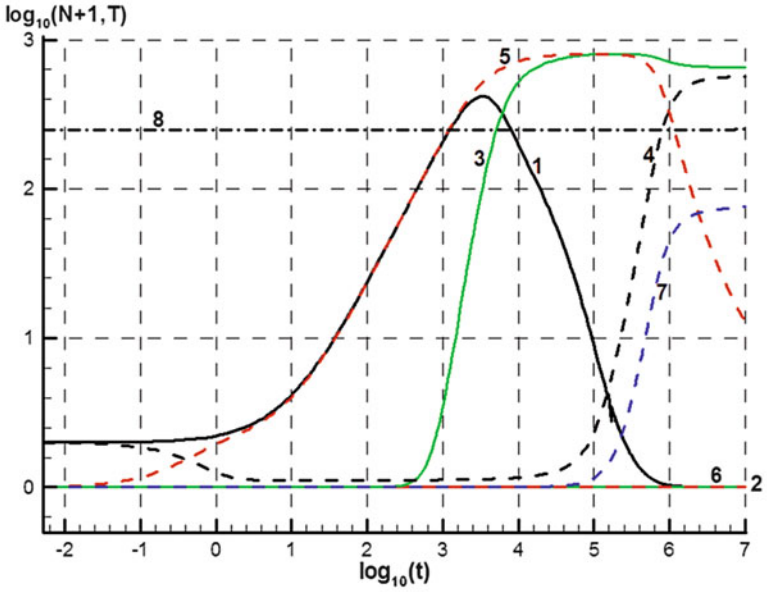


**Fig. 2.20** Numerical solution by the full model at zero electrical field at altitude $h = 60$ km (variant 4). *1* $N_{O_2^+}$, *2* $N_{N_2^+}$, *3* $N_{NO^+}$, *4* $N_e$, *5* $N_{O_2^-}$, *6* $N_{O^-}$, *7* $N_{O_3^-}$, and *8* gas temperature *T*. Scales over axes: *N* $cm^{-3}$, *t* s, *T* K

density and increase velocity of fast-particle ionization *W*/*N* per one particle. Data regarding the composition of background plasma obtained numerically agrees with the known literature (Brasseur and Solomon 1984; Ardelyan et al. 2013a).

## 2.5 Conclusion

In this chapter, we carried out a qualitative and quantitative analysis of prebreakdown and breakdown processes under an influence of external electric fields in the atmosphere at altitudes of 0 to 100 m. Simple qualitative models of the processes leading to prebreakdown and breakdown phenomena were presented. Detailed analysis revealed necessary features of the complex processes leading to the breakdown phenomena in air, the limitations of the qualitative models, and the approach one must follow to model the electric breakdown phenomena in air with the use of gas discharges.

Analysis showed that the phenomenon of air breakdown consists of several stages that are differently realized with respect to the altitude over the Earth. These stages can be accompanied by local gas heating, which can lead to unusual and unexpected behavior of plasma at high altitudes. These unexpected behaviors

should be taken into account when investigating high-altitude discharges and in the planning of high-altitude experiments using the application of gaseous discharges.

**Acknowledgments** The authors acknowledge L.P. Grachev for important formulation of ionization problems and fruitful discussions. The work was partially supported by grant RFBR 12-07-00654.

## References

Akishev YS, Deriugin AA, Karal'nik VB, Kochetov IV, Napartovich AP, Trushkin NI (1994) Experimental studies and numerical simulation of glow constant current discharge of atmospheric pressure. Fizika Plasmy 20(N.6):571–584

Aleksandrov NL (1988) Three-body attachment of electron to molecule. Uspekhi Fizich Nauk 154:177–206

Aleksandrov NL, Konchakov AM, Son EE (1978) Electron distribution function and kinetic coefficients of the nitrogen plasma. Fizika Plasmy 4(N.5):1182–1187

Aleksandrov AF, Bychkov VL, Grachev LP, Esakov II, Lomteva AY (2008) Effective ionization of air and oxygen in a near critical electric field at high pressures. Russ J Chem Phys B 2 (N.1):1–6

Aleksandrov AF, Bychkov VL, Volkov SA (2011) Breakdown characteristics of air in the lower atmosphere. Moscow Univ Phys Bull 66(N.1):88–91

Alexandrov NL, Vysikailo FI, Islamov RS, Kochetov IV, Napartovich AP, Pevgov VG (1981) Electron distribution function in mixture $N_2$:$O_2$ = 4:1. Teplofizika Vysokikh Temperature 19(N.1):22–27

Ardelyan N, Bychkov V, Kosmachevskii K, Chuvashev S, Malmuth N (2001) Modeling of plasmas in electron beams and plasma jets. In: Proceedings of 32-nd AIAA plasmadynamics and lasers conference and 4th weakly ionized gases workshop, Anaheim, CA, 11–14 June 2001. AIAA 2001-3101

Ardelyan NV, Bychkov VL, Bychkov DV, Denisiuk SV, Kosmachevskii KV (2012a) Non self-maintained discharge for flammable gas impact. Khimicheskaya Fizika 31(N.2):48–60

Ardelyan NV, Bychkov VL, Volkov SA et al (2012b) Mesospheric air breakdown characteristics. In: AIS-2012. Atmosphere, ionosphere, safety, Kaliningrad, 24–30 June 2012, pp 107–109

Ardelyan NV, Bychkov VL, Bychkov DV, Kosmachevskii KV (2013a) Electron-beam and non-self-maintained plasmas for PAC. In: Matveev IB (ed) Plasma assisted combustion, gasification and pollution control, vol 1. Outskirts Press, Denver, pp 183–372

Ardelyan NV, Bychkov VL, Kosmachevskii KV, Volkov SA et al (2013b) Air breakdown characteristics at high altitudes. AIAA-2013-0927. In: 51st AIAA Aerospace Sciences meeting, 7–10 Jan 2013, Grapewine, TX

Brasseur G, Solomon S (1984) Aeronomy of the middle atmosphere. D. Reidel Publishing Company, Dordrecht/Boston/Lancaster

Bychkov VL, Eletskii AV (1985) Electron beam plasma of high pressure. In: Smirnov BM (ed) Khimia plasmy, vol 12. Energoatomizdat Publishers, Moscow, pp 119–158

Bychkov VL, Grachev LP, Esakov II et al (2004) Longitudinal constant current electrical discharge in air supersonic flow. Techn Phys 48(N1):27–32

Bychkov V, Nikitin A, Dijkhuis G (2010) Modern state of ball lightning investigations. In: Bychkov VL, Golubkov GV, Nikitin AI (eds) The atmosphere and ionosphere: dynamics, processes and monitoring. Springer, Dordrecht/Heidelberg/London/New York, pp 201–373

Deminsky MA, Chernysheva IV, Umansky SY, Strelkova MI, Baranov AE, Kochetov IV, Napartovich AP et al (2013) Low temperature inflammation of methane-air mixture under an influence of non-equilibrium plasmas. Khimicheskaya Fizika 32:24–38

Dutton J (1975) A survey of electron swarm data. J Phys Chem Ref Data 4:577–856
Dyatko NA, Kochetov IV, Napartovich AP (1992) Electron energy distribution function in a decaying nitrogen plasma. Sov J Plasma Phys 18:462–468
Frost LS, Phelps AV (1962) Rotational excitation and momentum transfer cross sections for electrons in $H_2$ and $N_2$ from transport coefficients. Phys Rev 127:1621
Gallagher JW, Beaty EC, Dutton J, Pitchford LC (1983) An annotated compilation and appraisal of electron swarm data in electronegative gases. J Phys Chem Ref Data 12:109–152
http://www.lxcat.laplace.univ-tlse.fr/
Huxley LGH, Crompton RW (1974) The diffusion and drift of electrons in gases. Wiley, New York/London/Sidney/Toronto
Ionin AA, Kochetov IV, Napartovich AP, Yuryshev NN (2007) Physics and engineering of singlet delta oxygen production in low-temperature plasma. J Phys D 40:R25
Islamov RS, Kochetov IV, Pevgov VG (1977) Analysis of processes of electrons interaction with the molecule of the oxygen. Preprint FIAN №169, Moscow
Itikawa Y, Mason N (2005) Cross sections for electron collisions with water molecules. J Phys Chem Ref Data 34:1–22
Khodataev KV (2013) Discharge processes in a stratosphere and mesosphere during a thunderstorm. In: Bychkov VL, Golubkov GV, Nikitin AI (eds) The atmosphere and ionosphere: dynamics, processes and monitoring. Springer, Heidelberg/London/New York, pp 221–250
Kochetov IV, Naumov VG, Pevgov VG, Shashkov VM (1979) Direct heating mechanism of a $CO_2$–$N_2$–He laser mixture in a nonself-sustained discharge. Sov J Quantum Electron 6:847
Konovalov VP, Son EE (1987) Electron degradation spectra in gases. In: Smirnov BM (ed) Plasma chemistry. Energoatomizdat Publishers, Moscow, pp 194–227
Korn GA, Korn TM (1968) Mathematical handbook for scientists and engineers. McGraw Hill Inc., New York
Kossyi IA, Kostinsky AY, Matveev AA, Silakov VP (1992) Kinetic scheme of the non-equilibrium discharge in nitrogen-oxygen mixtures. Plasma Source Sci Technol 1 (N.3):207–220
Maetzing H (1991) Chemical kinetics of flue gas cleaning by irradiation with electrons. In: Prigogine I, Rice SA (eds) Advances in chemical physics, vol LXXX. Wiley, New York. ISBN 0-471-53281-9
Mnatsakanyan AK, Naidis GV (1991) Charged particle production and loss processes in nitrogen – oxygen plasmas. In: Smirnov BM (ed) Reviews of plasma chemistry. Consultants Bureau, New York, pp 259–292
Napartovich AP, Kochetov IV (2011) The value of swarm data for practical modeling of plasma devices. Plasma Source Sci Technol 20:025001
Nielsen RA, Bradbury NE (1937) Electron and negative ion nobilities in oxygen, air, nitrous oxide and ammonia. Phys Rev 51:69–75
Oksyuk YD (1965) Excitation of rotation levels of two-atomic molecules at electron collisions in the adiabatic approximation. JETP 49(N.4(10)):1261–1273
Petrović ZL, Dujko S, Marić D, Malović G, Nikitović Ž, Šašić O, Jovanović J, Stojanović V, Radmilović-Radenović M (2009) Measurement and interpretation of swarm parameters and their application in plasma modeling. J Phys D 42:194002
Phelps AV, Pitchford LC (1985) Anisotropic scattering of electrons by $N_2$ and its effects on electron transports: tabulations of cross section and results. 26-th report, JILA Information Center Report. University of Colorado, Boulder, CO
Raizer YP (1991) Gas discharge physics. Springer, Berlin
Raizer YP, Milikh GM, Shneider MN, Novakovski SV (1998) Long streamers in the upper atmosphere above thundercloud. J Phys D 31:3255–3264
Roznerski W, Leja K (1984) Electron drift velocity in hydrogen, nitrogen, oxygen, carbon monoxide, carbon dioxide and air at moderate E/N. J Phys D 17:279–285
Sedunov YS (ed) (1991) Atmosphere. Reference book. Gidtometeoizdat, Leningrad
Shkarovsky IP, Johnston TW, Bachynski MP (1966) The particle kinetics of plasma. Addison-Wesley Publishing Company, Boston/Palo Alto/London/Don Mills

Smirnov BM (1974) Ions and excited atoms in plasmas. Atomizdat, Moscow
Smith K, Thomson RM (1978) Computer modeling of gas lasers. Plenum Press, New York/London
Virin LI, Dzhatspanyan RV, Karachevtsev GV, Potapov VK, Tal'rose VL (1979) Ion-molecule reactions in gases. Nauka, Moscow
Wahlin L (1994) Elements of fair weather electricity. J Geophys Res 99(N.D5):10767
Yousfi M, Azzi N, Segur P et al (1987) Electron-molecule collision cross sections and Electron swarm parameters in some atmospheric gases ($N_2$, $O_2$, and $H_2O$). Center de Physique Atomique de Toulouse & Instituto di Electtrotecnica ed Electronica. Universita di Padova, pp 1
Zadorozhny AM, Tyutin AA (1998) Effects of geomagnetic activity on the mesospheric electric fields. Ann Geophys 16:1544–1551

http://www.springer.com/978-3-319-05238-0

The Atmosphere and Ionosphere
Elementary Processes, Monitoring, and Ball Lightning
Bychkov, V.L.; Golubkov, G.V.; Nikitin, A.I. (Eds.)
2014, XVIII, 386 p. 136 illus., 70 illus. in color.,
Hardcover
ISBN: 978-3-319-05238-0